

# Quantum Chemical Calculations for some Isatin Thiosemicarbazones

Fatma Kandemirli<sup>\*,\*\*</sup> et al.  
*Niğde University,  
Turkey*

## 1. Introduction

Derivatives of isatin are reported to be present in mammalian tissues and body fluids (Casas et al., 1996; Agrawal & Sartorelli, 1978; Casas et al., 1994; Medvedev et al., 1998; Boon, 1997; Pandeya & Dimmock, 1993; Rodriguez-Argüelles et al., 1999; Casas et al., 2000) and possess antibacterial (Daisley & Shah, 1984), antifungal (Piscopo et al., 1987), and anti-HIV (Pandeya et al., 1998, 1999) activities. *N*-methylisatin- $\beta$ -4', 4' - diethylthiosemicarbazone were also reported to have activity against the viruses such as cytomegalo and moloney leukemia viruses (Sherman et al., 1980; Ronen et al., 1987). With the help of combinatorial method, the cytotoxicity and antiviral activities of isatin- $\beta$ -thiosemicarbazones against the vaccine virus and cowpox virus-infected human cells were evaluated (Pirrung et al., 2005).

Some 5-fluoroisatin, 5-fluoro-1-morpholino/piperidinomethyl, and 5-nitroisatin synthesized. They are reported to have anti-TB activity. ETM Study has also been carried out on these compounds (Karali et al., 2007). Synthesis and quantum chemical calculations of 5-methoxyisatin-3-(*N*-cyclohexyl), its Zn (II) and Ni (II) complexes (Kandemirli et al., 2009a), and 5-methoxyisatin-3-(*N*-cyclohexyl)thiosemicarbazone (Kandemirli et al., 2009b) were studied. The thiosemicarbazones likely possess anti-HIV activity according to 3D pharmacophoric distance map analysis (Bal et al., 2005).

Isatin-thiosemicarbazones may coordinate through the deprotonated nitrogen atom, sulphur atom of thiosemicarbazone group, and carbonyl oxygen atom with the metal, depending on its nature. Zinc (II) and mercury (II) complexes of isatin-3-thiosemicarbazones were reported to be coordinated through imino nitrogen and thiolato sulfur atoms and was suggested to have tetrahedral structures (Akinchan et al., 2002).

It was reported that only amino nitrogen atom coordinates in the Cu (II) complex (Ivanov et al., 1988). Quantum chemical calculations and IR studies on Zn (II) and Ni (II) complexes of

---

\* M. Iqbal Choudhary<sup>2</sup>, Sadia Siddiq<sup>2</sup>, Murat Saracoglu<sup>3</sup>, Hakan Sayiner<sup>4</sup>,  
Taner Arslan<sup>5</sup>, Ayşe Erbay<sup>6</sup> and Baybars Köksoy<sup>6</sup>

<sup>2</sup>University of Karachi, Pakistan,

<sup>3</sup>Erciyes University, Turkey,

<sup>4</sup>Kahita State Hospital, Turkey,

<sup>5</sup>Osmangazi University, Turkey, Turkey,

<sup>6</sup>Kocaeli University, Turkey

\*\*Corresponding Author

5-fluoro-isatin -3-(*N*-benzylthiosemicarbazone) have recently been reported (Gunesdogdu-Sagdinc et al., 2009).

During the current study, we prepared [Zn(HICHT)<sub>2</sub>], [Zn(HMIPT)<sub>2</sub>], [Zn(HIPT)<sub>2</sub>], [Zn(HICPT)<sub>2</sub>], [Zn(HIBT)<sub>2</sub>], [Ni(HMIPT)<sub>2</sub>], [Ni(HIPT)<sub>2</sub>], [Ni(HICPT)<sub>2</sub>], [Ni(HIBT)<sub>2</sub>], and [Ni(HICHT)<sub>2</sub>] derivatives, and characterized them with elemental analysis, and IR, UV, and <sup>1</sup>H-NMR spectroscopic techniques.

In view of the reports about antimicrobial and antifungal activities of the isatin derivatives, we synthesized and screened compounds **1-16** (Table 1) for their antimicrobial effects in vitro against *Bacillus subtilis*, *Escherichia coli*, *Staphylococcus aureus*, *Shigella flexnari*, *Pseudomonas aeruginosa*, and *Salmonella typhi* bacterial strains and *Aspergillus flavus*, *Candida albicans*, *Microsporum canis*, *Fusarium solani*, and *Candida glabrata* fungal strains. Compounds **1**, **14**, and **16** were found to be moderately active, compounds **2**, and **4** possess a good activity, while compound **13** exhibited a significant activity against *Microsporum canis*. Compounds **13**, **12**, and **4** exhibited moderate activities against *Fusarium solani*. Compound **10** showed a moderate activity against *Candia albicans*. Compound **5** was only moderately active against the *Candida albicans*.

Compound No	List of the Compounds
1	5-Methoxyisatin-3-( <i>N</i> -cyclohexyl) thiosemicarbazone (H <sub>2</sub> MICT)
2	5-Methoxyisatin-3-( <i>N</i> -benzyl)thiosemicarbazone (H <sub>2</sub> MIBT)
3	5-Methoxyisatin-3-( <i>N</i> -phenyl)thiosemicarbazone (H <sub>2</sub> MIPT)
4	5-Methoxyisatin-3-( <i>N</i> -chlorophenyl)thiosemicarbazone (H <sub>2</sub> MICPT)
5	Isatin-3-( <i>N</i> -cyclohexyl)thiosemicarbazone(H <sub>2</sub> ICHT)
6	[Zn(HICHT) <sub>2</sub> ]
7	[Zn((HMICT) <sub>2</sub> )]
8	[Zn(HMIPT) <sub>2</sub> ]
9	[Zn(HIPT) <sub>2</sub> ]
10	[Zn(HICPT) <sub>2</sub> ]
11	[Zn(HIBT) <sub>2</sub> ]
12	[Ni((HMICHT) <sub>2</sub> )]
13	[Ni(HMIPT) <sub>2</sub> ]
14	[Ni(HIPT) <sub>2</sub> ]
15	[Ni(HICPT) <sub>2</sub> ]
16	[Ni(HIBT) <sub>2</sub> ]
17	[Ni(HICHT) <sub>2</sub> ]
18	Isatin-3-( <i>N</i> -benzyl)thiosemicarbazone (H <sub>2</sub> IBT)
19	Isatin-3-( <i>N</i> -phenyl)thiosemicarbazone (H <sub>2</sub> IPT)
20	Isatin-3-( <i>N</i> -chlorophenyl)thiosemicarbazone (H <sub>2</sub> ICPT)

Table 1. Studied compounds

## 2. Experimental

Elemental analyses were performed by using a LECO CHN Elemental Analyzer. IR Spectra were recorded by Shimadzu FT-IR 8201 spectrometer with the KBr technique in the region of 4000-300  $\text{cm}^{-1}$ , which was calibrated by polystyrene. There was no decomposition of the samples due to the effect of potassium bromide. The  $^1\text{H-NMR}$  spectra were recorded in  $\text{DMSO-}d_6$  on a BRUKER DPX-400 (400 MHz) spectrometer.

The ligands under study were obtained by refluxing an ethanolic solution of 4-cyclohexyl-3-thiosemicarbazide, 4-benzyl-3-thiosemicarbazide, 4-phenyl-3-thiosemicarbazide, and 4-(4-chlorophenyl)-3-thiosemicarbazide with isatin (1H-indole-2,3-dione) or 5-methoxyisatin (all were purchased from Aldrich Chemical Company USA and used without purification), as described in the literature (Karali et al., 2007; Kandemirli et al., 2009a, 2009b).

### 2.1 General procedure for synthesis of Ni and Zn complexes

1 mmol of appropriate ligand was dissolved in 20 mL of ethanol at 50-55  $^{\circ}\text{C}$  and then slowly added to ethanol solution (10 mL) of 0.5 mmol zinc acetate dihydrate or nickel acetate tetrahydrate. The mixture was refluxed for 2 h for nickel complex, and 6 h for zinc complex at approximately 75  $^{\circ}\text{C}$ . The zinc complex precipitated at the end of the reflux, while the nickel complex precipitated only after two days of stirring. The solid was filtered, washed with ethanol, and diethyl ether, and dried under vacuum.

#### 2.1.1 $[\text{Zn}(\text{HICHT})_2]$ (6)

Yield: (80%). (M.p.: 288-290  $^{\circ}\text{C}$ )

$^1\text{H-NMR}$  ( $\text{DMSO-}d_6$ , ppm):  $\delta$  1-2 (cyclohexyl C-H), 4.11 (m, cyclohexyl C-H), 6.90-8.3 (aromatic C-H), 8.95 (d,  $J = 7.8$  Hz), NH 10.80 (s, indole-NH)

IR ( $\text{cm}^{-1}$ ): 1688 (C=O), 1595 (C=N), 819 (C=S)

Calculated: % C: 53.92, % H: 5.128, % N: 16.77, % S: 9.60, found: % C: 53.49, % H: 5.644, % N: 16.06, % S: 9.58.

#### 2.1.2 $[\text{Zn}(\text{HMIPT})_2]$ (8)

Yield: (64%). (M.p.: 320  $^{\circ}\text{C}$ )

$^1\text{H-NMR}$  ( $\text{DMSO-}d_6$ , ppm):  $\delta$  3.35 (s,  $\text{CH}_3$ -methoxy), 6.91-7.72 (aromatic C-H), 10.76 (s, NH), 11.04 (s, indole-NH)

IR ( $\text{cm}^{-1}$ ): 1697 (C=O), 1589 (C=N), 817 (C=S)

Calculated: % C: 53.67, % H: 3.66, % N: 15.64, % S: 8.95, found: % C: 53.64, % H: 3.65, % N: 15.67, % S: 9.08.

#### 2.1.3 $[\text{Zn}(\text{HIPT})_2]$ (9)

Yield: (90%). (M.p.: 310  $^{\circ}\text{C}$ )

$^1\text{H-NMR}$  ( $\text{DMSO-}d_6$ , ppm):  $\delta$  7.01-8.11 (aromatic C-H), 10.68 (s, NH), 11.01 (s, indole-NH)

IR (cm<sup>-1</sup>): 1703 (C=O), 1595 (C=N), 802 (C=S)

Calculated: % C: 54.92, % H: 3.38, % N: 17.08, % S: 9.77, found: % C: 54.52, % H: 3.31, % N: 16.91, % S: 10.10.

#### 2.1.4 [Zn(HICPT)<sub>2</sub>] (10)

Yield: (82%) (M.p.: 321 °C)

<sup>1</sup>H-NMR (DMSO-*d*<sub>6</sub>, ppm): δ 7.03-8.08 (aromatic C-H), 10.73 (s, NH), 11.06 (s, indole-NH)

IR (cm<sup>-1</sup>): 1695 (C=O), 1600 (C=N), 816 (C=S)

Calculated: % C: 48.69, % H: 2.78, % N: 15.45, % S: 8.84, found: % C: 48.43, % H: 3.03, % N: 14.96, % S: 8.81.

#### 2.1.5 [Zn(HIBT)<sub>2</sub>] (11)

Yield: (79%) (M.p.: 318 °C)

<sup>1</sup>H-NMR (DMSO-*d*<sub>6</sub>, ppm): δ 4.80 (d, benzyl-CH<sub>2</sub>), 6.95-7.40 (aromatic C-H), 9.45 (t, *J*=7.52 Hz), NH), 10.81 (s, indole-NH).

IR (cm<sup>-1</sup>): 1690 (C=O), 1599 (C=N), 814 (C=S)

Calculated: % C: 56.18, % H: 3.83, % N: 16.38, % S: 9.37, found: % C: 55.72, % H: 3.79, % N: 16.24, % S: 9.58.

#### 2.1.6 [Ni(HMIPT)<sub>2</sub>] (13)

Yield: (90%) (M.p.: 300 °C)

IR (cm<sup>-1</sup>): 1670 (C=O), 1589 (C=N), 818 (C=S),

Calculated: % C: 54.17, % H: 3.69, % N: 15.79, % S: 9.04, found: % C: 54.00, % H: 3.73, % N: 15.71, % S: 9.07.

#### 2.1.7 [Ni(HIPT)<sub>2</sub>] (14)

Yield: (81%) (M.p.: 296 °C)

IR (cm<sup>-1</sup>): 1660 (C=O), 1595 (C=N), 802 (C=S),

Calculated: % C: 52.48, % H: 3.41, % N: 16.25, % S: 9.87, found: % C: 52.79, % H: 3.60, % N: 16.24, % S: 9.33.

#### 2.1.8 [Ni(HICPT)<sub>2</sub>] (15)

Yield: (70%) (M.p.: 265-267 °C)

IR (cm<sup>-1</sup>): 1672 (C=O), 1595 (C=N), 817 (C=S)

Calculated: % C: 51.16, % H: 2.80, % N: 15.59, % S: 8.92, found: % C: 51.37, % H: 3.08, % N: 15.71, % S: 8.63.

### 2.1.9 [Ni(HIBT)<sub>2</sub>] (16)

Yield (84%) (M.p.: 265-267 °C)

IR (cm<sup>-1</sup>): 1659 (C=O), 1595 (C=N), 818 (C=S)

Calculated: % C: 56.73, % H: 3.86, % N: 16.54, % S: 9.46, found: % C: 56.35, % H: 3.84, % N: 16.40, % S: 9.60.

### 2.1.10 [Ni(HICHT)<sub>2</sub>] (17)

Yield: (90%). (M.p.: 265 °C)

IR (cm<sup>-1</sup>): 1664 (C=O), 1595 (C=N), 823 (C=S)

Calculated: % C: 53.47, % H: 5.18, % N: 16.54, % S: 9.69, found: % C: 52.99, % H: 5.17, % N: 16.14, % S: 9.37.

## 2.2 Antibacterial activity

The antibacterial activities were determined by using the agar well diffusion method (Rahman et al., 2001). The wells were dugged in the media with a sterile borer and an eight-hour-old bacterial inoculum containing 0>ca. 104-106 colony forming units (CFU)/mL were spread on the surface of the nutrient agar. The recommended concentration of the test sample (2 mg/mL in DMSO) was introduced into the respective wells. Other wells containing DMSO and the reference antibacterial drug imipenem served as negative and positive controls, respectively. The plates were incubated immediately at 37 °C for 20 h. The activity was determined by measuring the diameter of the inhibition zone (in mm), showing complete inhibition. Growth inhibition was calculated with reference to the positive control.

## 2.3 Antifungal assay

To test for antifungal activity, the agar dilution method, a modification of the agar dilution method of Washington and Sutter (1980), was employed (Ajaiyeoba et al., 1988). Test tubes having sterile SDA were inoculated with test samples (200 mg/mL), and kept in a slanting position at room temperature. Test fungal culture was inoculated on the slant and growth inhibitions were observed after an incubation period of 7 days at 27 °C. Control agar tubes were made in parallel and treated similarly, except for the presence of test sample. Growth inhibition was calculated with reference to positive control.

## 2.4 Theoretical and computational details

All the quantum chemical calculations on the compounds **18**, **5**, **19**, and **20** were performed with full geometrical optimizations by using standard Gaussian 03 and 09 software package (Frisch et al., 2004). Geometrical optimization were carried out with two different methods, *ab initio* methods at the Hartree-Fock (HF) level, and density functional theory (DFT) by using the B3LYP change-correlation corrected functional (Becke, 1993; Lee et al., 1988) with 6-31G(d,p), 6-311G(d,p), 6-311++G(d,p), LANL2DZ 6-31G(d,p) basis sets, and BP86/CEP-31G\* hybrid functional with 30% HF exchange and Stevens-Basch-Krauss pseudo potentials with polarized split valence basis sets (CEP-Compact Effective Potentials -31G\*) (Hill et al., 1992; Stevens et al., 1984).

Fukui functions, which are common descriptors of site reactivity and can be expressed by the following equations, were calculated by AOMix program (Gorelsky, 2009; Gorelsky & Lever, 2001).

$$f_k^+ = \rho_k(N+1) - \rho_k(N) \text{ (for nucleophilic attack)}$$

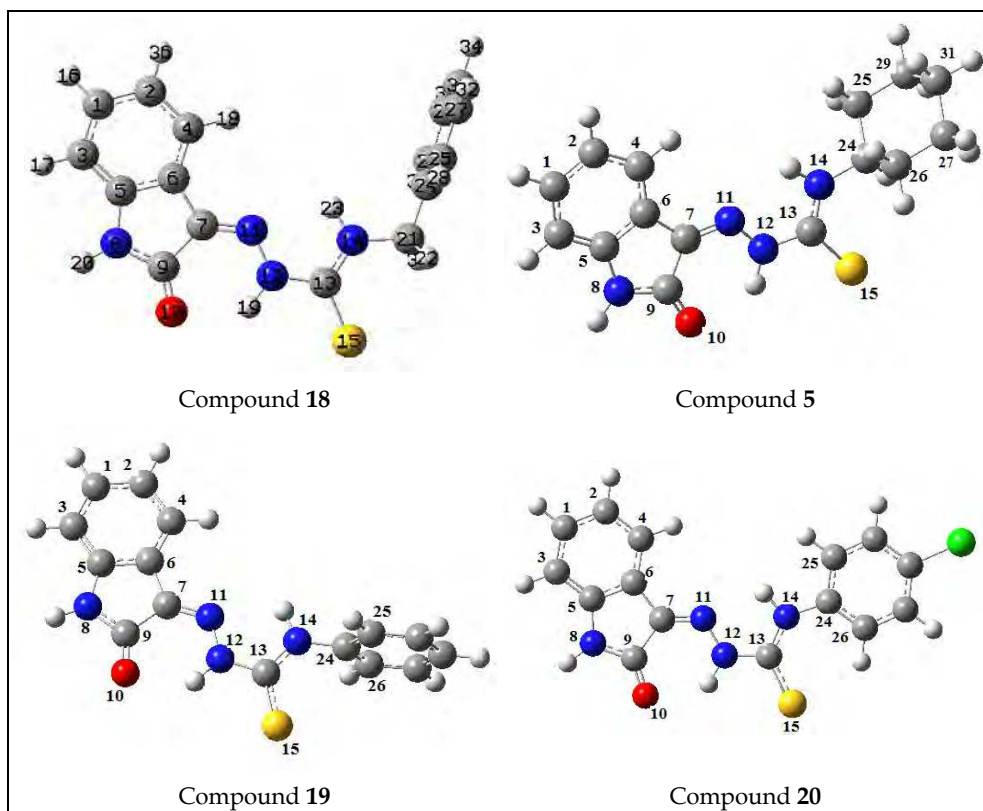
$$f_k^- = \rho_k(N) - \rho_k(N-1) \text{ (for electrophilic attack)}$$

$$f_k^o = \rho_k(N+1) - \rho_k(N-1)/2 \text{ (for radical attack)}$$

Where,  $k$  represents the sites (atoms/molecular fragments) for nucleophilic, electrophilic and radical agents and  $\rho_k$  are their gross electron populations. An elevated value of  $f_k$  implies a high reactivity of the site  $k$ .

### 3. Results and discussion

The optimized structures of the compounds **18**, **5**, **19**, and **20** ligands, and the optimized structures of their corresponding Ni(II) and Zn(II) complexes are shown in Figure 1.



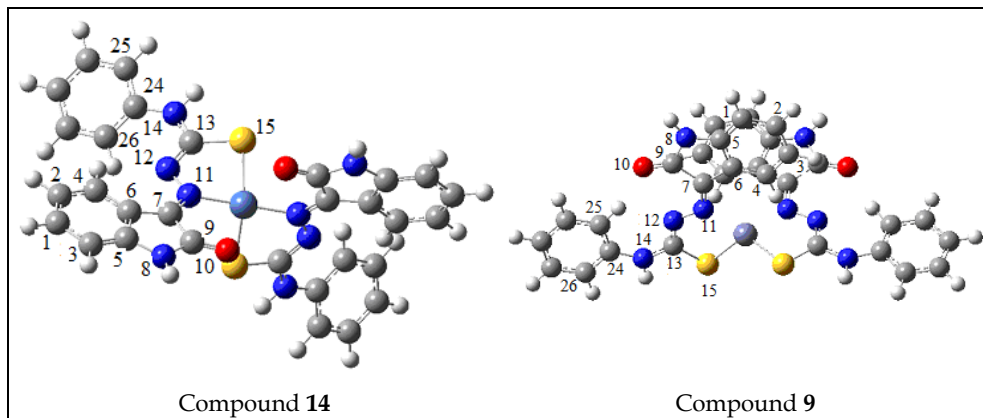


Fig. 1. Optimized structures of compounds 18, 5, 19, 20, 14, 9

Values of the optimized geometrical parameters for all compounds are presented in Tables 2 and 3. The bond lengths, bond angles, and dihedral angles for compounds 18, 5, 19, and 20 are almost the same as in isatin group. Mulliken charges of most atoms, except N and S, belong to thiosemicarbazone group are the same value. Therefore comparison among ligands, and deprotonated forms of ligand and complexes were made for compound 19. In the deprotonated forms of 19, as in N11-N12, C6-C7, and C13-C14, the bond lengths decrease, while C7-C9, C5-N8, and C4-C6 bond lengths increase. In Zn (II) complexes, C4-C6, C6-C7 bond lengths are similar to those of ligands. N11-N12 bond length in the deprotonated form of the ligands decreases, whereas in the complexes this bond length increases due to a transfer of charge from N atoms to metal. In the complex form, C-S bond length increases from 1.667 Å to 1.759 Å in Ni (II) complex, and 1.744 Å in Zn (II) complex.

The calculated bond lengths of the Zn-S and Zn-N bonds for compound 9 were found to be 2.323 and 2.107 Å. The bond lengths of the Ni-N and Ni-S, Ni-O bonds for compound 14

Atoms	Compounds						
	18	5	20	19	19 <sup>a</sup>	9	14
Bond distances (Å)							
C1-C2	1.396	1.396	1.396	1.396	1.408	1.396	1.395
C1-C3	1.399	1.399	1.399	1.399	1.396	1.398	1.399
C2-C4	1.396	1.396	1.395	1.395	1.382	1.393	1.396
C3-C5	1.385	1.385	1.385	1.385	1.385	1.386	1.385
C4-C6	1.390	1.390	1.390	1.390	1.406	1.393	1.394
C5-C6	1.411	1.411	1.411	1.411	1.424	1.413	1.417
C6-C7	1.456	1.456	1.455	1.456	1.418	1.455	1.450
C7-C9	1.502	1.502	1.503	1.502	1.548	1.525	1.502

C5-N8	1.403	1.403	1.403	1.403	1.391	1.392	1.394
N8-C9	1.380	1.380	1.378	1.379	1.380	1.387	1.388
C7-N11	1.296	1.296	1.295	1.296	1.299	1.310	1.307
N11-N12	1.332	1.332	1.333	1.333	1.283	1.347	1.350
N12-C13	1.391	1.393	1.395	1.391	1.389	1.326	1.331
C13-S15	1.673	1.676	1.669	1.667	1.661	1.759	1.744
C13-N14	1.339	1.340	1.353	1.348	1.325	1.360	1.348
N14-C21	1.463	1.462	1.407	1.432	1.425	1.412	1.348
C21-C24	1.511	-	-	-	-	-	-
C24-C25	1.398	1.538	1.404	1.393	1.399	1.405	1.534
C24-C26	1.398	1.535	1.399	1.393	1.398	1.400	1.539
S15-Zn	-	-	-	-	-	2.323	2.259
N11-Zn	-	-	-	-	-	2.107	1.903
O10-Ni	-	-	-	-	-	-	2.830
Bond angles (°)							
C5-C6-C7	106.79	106.80	106.76	106.78	106.83	107.33	106.42
C6-C7-C9	107.02	107.00	107.01	107.01	107.29	106.47	107.54
C5-N8-C9	111.81	111.82	111.79	111.81	111.65	112.60	111.87
N8-C9-O10	126.91	126.87	105.29	105.29	104.17	124.43	126.18
C7-C9-O10	127.80	127.84	127.64	127.77	126.50	131.09	129.00
C7-N11-N12	119.25	119.25	119.33	119.29	126.94	116.83	117.32
C9-C7-N11	126.46	126.46	126.29	126.46	123.14	126.33	120.51
N11-N12-C13	120.79	121.01	121.47	120.93	116.34	117.34	112.11
N12-C13-S15	33.46	118.35	117.54	27.38	102.33	128.18	112.11
S15-C13-N14	125.98	127.13	130.01	126.98	135.52	113.71	118.44
C13-N14-C21	123.87	125.55	132.89	125.18	127.50	133.38	125.44
N14-C21-C24	110.10	109.87	115.97	119.79	117.49	115.70	109.61
C13-Zn/Ni-N11	-	-	-	-	-	91.80	90.93
S15- Zn/Ni -N11	-	-	-	-	-	130.33	95.84
N11- Zn/Ni -S15	-	-	-	-	-	123.82	84.44
O10-Ni-S15	-	-	-	-	-	-	79.44
O10-Ni-O1	-	-	-	-	-	-	74.20
O10-Ni-N11	-	-	-	-	-	-	73.70

<sup>a</sup> Protonated form of 19

Table 2. Selected bond distances (Å) and bond angles charges calculate with B3LYP/6-311G(d,p) for compounds **18**, **5**, **20**, **19**, **9**, and **14**



were 2.259, 1.903, and 2.830 Å, respectively. Experimental data of Ni-N and Ni-S, Ni-O bonds for the crystallographic analyses of complex of isatin- $\beta$ -thiosemicarbazone were 2.023, 2.368, and 2.226 Å, respectively. The calculated dihedral angles  $\angle$ C6-C7-N11-N12 and  $\angle$ N12-C13-N14-C21 for compound **19** were 179.98° and -180.00°, respectively, very close to the crystal values of 5-methoxyisatin-3-(*N*-cyclohexyl)thiosemicarbazone) (Kandemirli et al., 2009a).

Atoms	Compounds						
	18	5	20	19	19 <sup>a</sup>	9	14
Dihedral angles (°)							
C3-C5-N8-C9	-180.00	179.96	-	-179.99	-176.17	-	-
C5-C6-C7-N11	-180.00	-179.87	180.00	179.99	-178.71	176.47	-178.31
C5-N8-C9-O10	180.00	179.98	180.00	-179.98	176.75	179.62	175.86
N8-C9-C7-N11	180.00	179.85	-180.00	-179.98	-155.39	-176.13	179.37
C6-C7-N11-N12	-180.00	179.96	180.00	-179.98	28.48	177.24	1.70
C9-C7-N11-N12	0.00	0.08	0.00	0.01	-4.73	-5.54	-174.73
O10-C9-C7-N11	0.00	-0.07	0.00	-0.023	-147.12	2.76	1.58
C7-N11-N12-C13	-180.00	-179.78	-180.00	-179.99	123.93	176.10	160.68
N11-N12-C13-S15	180.00	179.55	-180.00	-180.00	-172.93	-3.78	-3.65
N12-C13-N14-C21	180.00	177.56	-179.98	-180.00	8.06	-0.22	-6.96
S15-C13-N14-C21	0.00	-2.69	0.02	0.00	-38.29	-179.42	176.54
C13-N14-C21-C24	179.99	-	-	-	-	-	-
N14-C21-C24-C25	89.51	-92.75	179.96	-91.29	142.56	5.42	156.43
N14-C21-C24-C26	-89.48	143.32	-0.04	91.24	142.56	-175.30	-79.66
Mulliken charges (ē)							
C5	0.239	0.239	0.240	0.239	0.261	0.253	0.245
C6	-0.134	-0.133	-0.136	-0.134	-0.110	-0.157	-0.140
C7	0.081	0.082	0.094	0.084	0.142	0.203	0.205
N8	-0.489	-0.489	-0.489	-0.489	-0.483	-0.490	-0.489
C9	0.421	0.420	0.423	0.421	0.436	0.614	0.376
O10	-0.360	-0.359	-0.357	-0.359	-0.231	-0.412	-0.322
N11	-0.225	-0.228	-0.240	-0.231	-0.207	-0.605	-0.476
N12	-0.274	-0.273	-0.270	-0.270	-0.082	-0.352	-0.266
C13	0.226	0.228	0.229	0.215	0.145	0.329	0.205
S15	-0.237	-0.244	-0.208	-0.201	0.163	-0.572	-0.317
N14	-0.405	-0.392	-0.463	-0.437	-0.381	-0.537	-0.379
Zn or Ni	-	-	-	-	-	1.568	1.036

<sup>a</sup> Protonated form of 19

Table 3. Selected dihedral angles and Mulliken charges calculate with B3LYP/6-311G(d,p) for compounds **18**, **5**, **20**, **19**, **9**, and **14**

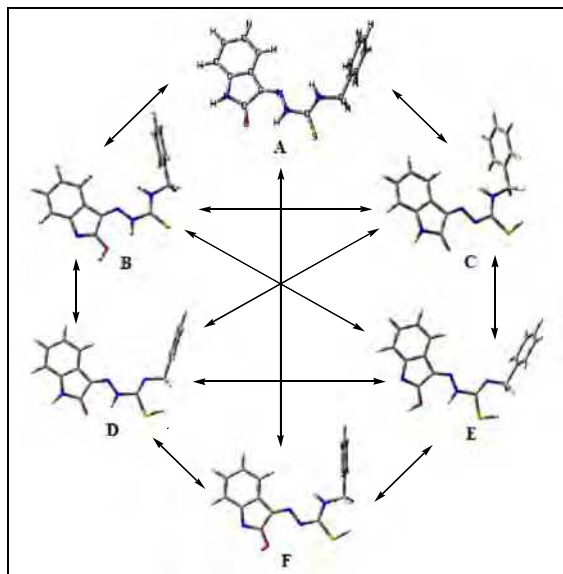


Fig. 2. Possible tautomeric forms for compound **18**

Calculated theoretical angle for **16** ( $\angle\text{C13-Ni-N11}$ ,  $\angle\text{S15-Ni-N11}$ ,  $\angle\text{N11-Ni-S15}$ ,  $\angle\text{O10-Ni-S15}$ ,  $\angle\text{O10-Ni-O1}$ ,  $\angle\text{O10-Ni-N11}$  were  $90.93^\circ$ ,  $95.84^\circ$ ,  $84.44^\circ$ ,  $79.44^\circ$ , and  $74.20^\circ$ , respectively), which indicated that the complex is in a distorted octahedral coordination. Two terdentate monodeprotonated thiosemicarbazone groups, each of which is attached to the metal with the sulfur, the nitrogen atom from the hydrazine chain, and the carbonylic oxygen of the isatin moiety. The calculated dihedral angles of  $\angle\text{C3-C5-N8-C9}$ ,  $\angle\text{C6-C7-N11-N12}$ ,  $\angle\text{N11-N12-C13-S15}$  were  $-179.99^\circ$ ,  $-179.98^\circ$ , and  $-180.00^\circ$  which showed that ligands are planar.

As presented in Table 3, Mulliken charges of C5, C6, N8, C9, and N12 were similar to each other in the neutral form. Most of the changes are on the N14 atom because of the changes in substituent attached to the N14 atom. The Mulliken charge of N14 atom was  $-0.405 \bar{e}$  for H<sub>2</sub>IBT,  $-0.392 \bar{e}$  for H<sub>2</sub>ICHT,  $-0.463 \bar{e}$  for H<sub>2</sub>IPT, and  $-0.437 \bar{e}$  for H<sub>2</sub>ICPT. Mulliken charges of atoms, both in the indole ring and thiosemicarbazone group, undergo a significant change, depending whether ligand is in the deprotonated form or in complexation process.

### 3.1 The possible tautomeric forms of ligands

The optimized structure for **18** ligand, calculated with B3LYP/6-311G(d,p), is shown in Figure 2. Electronic and zero point energies for compounds **18**, **5**, **19**, and **20** were given in Table 4. The most stable tautomeric form is A for studied ligands. In the form A, calculated electronic and zero point energy for compounds **18**, **5**, **19**, and **20** were  $-1310.525279 \text{ au}$ ,  $-1274.797093 \text{ au}$ ,  $-1271.228351 \text{ au}$ , and  $1730.859463 \text{ au}$ , respectively. Therefore, all discussions are based on A form.

Tautomeric forms	Compounds			
	18	5	19	20
A	-1310.525279	-1274.797093	-1271.228351	-1730.859463
B	-1310.516899	-1274.770217	-1271.201356	-1730.830654
C	-1310.505963	-1274.758544	-1271.196548	-1730.826130
D	-1310.492187	-1274.764865	-1271.207983	-1730.837828
E	-1310.463311	-1274.737477	-1271.179113	-1730.808789
F	-1310.466475	-1274.743568	-1271.175689	-1730.804186

Table 4. Electronic and zero point energy calculated with B3LYP/6-311G(d,p) for compounds **18**, **5**, **19**, and **20** ligands

### 3.2 Fukui functions

Fukui functions values for compounds **18**, **5**, **19**, and **20** calculated with B3LYP/6-31G(d,p) were summarized in Table 5. The contribution of sulphur atom to the HOMO is 90.2% and 89.52% for compounds **18**, and **5**, whereas, for compounds **19**, and **20**, the contribution of S decreases to 48.32%, and 41.90%, respectively. The other contributions for compound **19** comes from N14 atom (12.63%) belonging to thiosemicarbazone and phenyl groups (C24: 5.41%, C25: 5.65%, C25: 15%, C29: 1.93%, C25: 9.18%), and isatin group (C1: 1.49%, C5: 1.14%, C6: 1.06%, C7: 2.08%). For compound **5** contribution involves mostly N14 (13.45%), belonging to thiosemicarbazone group and phenyl ring (C24: 6.96%, C25: 5.75%, C25: 4.78%, C29: 2.76%, C25: 10.14%). Proportions of contribution change were according to the groups attached to N14 atom. Attaching phenyl group instead of cyclohexyl to N14 atom decreases the contribution of S atom to the HOMO orbital to approximately half.

Tauto. Forms*	For electrophilic attack													
	C1	C5	C6	C7	O10	N12	C13	N14	S 15	C24	C25	C26	C29	C31
A	-	-	-	-	-	1.06	4.26	-	90.20	-	-	-	-	-
B	-	-	-	-	-	1.35	4.09	-	89.52	1.12	-	-	-	-
C	1.49	1.14	1.06	2.08	1.10	2.05	-	12.63	48.32	5.41	5.65	4.15	1.93	9.18
D	-	-	-	1.20	-	-	-	13.45	41.90	6.96	5.75	4.78	2.76	10.14
	For nucleophilic attack													
	C 1	C 4	C5	C6	C7	N8	C9	O10	N11	N12	C13	N14	S15	-
A	6.69	5.03	3.98	3.61	12.92	1.46	10.45	8.96	26.63	5.35	4.45	2.16	6.98	-
B	6.71	5.05	3.98	3.64	12.90	1.44	10.40	8.94	26.68	5.44	4.42	2.14	6.89	-
C	6.52	5.01	3.94	3.26	13.23	1.39	9.95	8.70	25.21	4.57	5.39	1.86	8.12	-
D	6.51	5.05	3.97	3.15	13.51	1.39	9.90	8.70	24.87	4.23	5.66	1.79	8.28	-

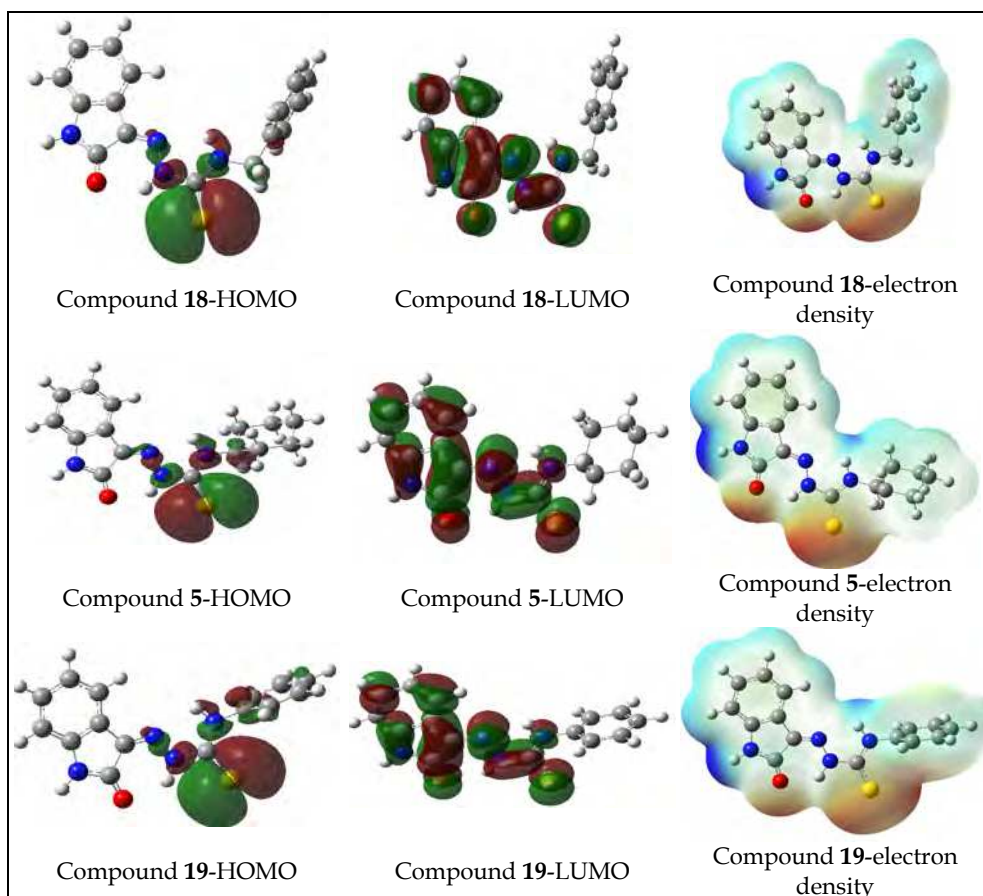
\* Tautomeric forms

Table 5. Fukui functions for calculated with B3LYP/6-31G(d,p) for compounds **18**, **5**, **19**, and **20** ligands

The other molecular parameters, obtained through the theoretical calculations by using the level of B3LYP and RHF theory by using 6-31G(d,p), 6-311G(d,p), 6-311++G(d,p) basis sets, are the  $E_{\text{HOMO}}$  (highest occupied molecular orbital), and the  $E_{\text{LUMO}}$  (lowest unoccupied molecular orbital). The highest occupied and the lowest unoccupied molecular orbital

energies ( $E_{\text{HOMO}}$  and  $E_{\text{LUMO}}$ ), and the five molecular orbital energies for the nearest frontier orbitals of compounds **18**, **5**, **19**, and **20** were presented in Table 6. HOMO and LUMO electron densities for compounds **18**, **5**, **19**, and **20** which are calculated with B3LYP/6-311++G(d,p) and shown in Figure 3.  $E_{\text{HOMO}}$  values, obtained with B3LYP method, are higher than those of RHF method. Calculated  $E_{\text{HOMO}}$  at the level of RHF/6-311G(d,p) and B3LYP/6-311G(d,p) theory are -0.30438 au and -0.21286 au for **18**; 0.30266 au and -0.21701 au for **5**; -0.30386 au and -0.21656 au for **19**; and -0.30899 au and -0.22050 au for compound **20**. HOMO of compounds **5**, **18**, and **19** consist of mainly S atom belonging to the thiosemicarbazone group, and HOMO of compound **20** includes mainly S and chlorophenyl group. LUMO orbitals are distributed mainly over isatin and thiosemicarbazone groups for compounds **18**, **5**, **19**, and **20**.

Electron densities for compounds **18**, **5**, **19**, and **20** are also shown in Figure 3. As shown in Figure 3, electron rich regions shown as red are found in the vicinity of the double bonded O and S atoms attached to C which belongs to isatin moiety and thiosemicarbazone moiety, respectively. Electron poor regions shown as blue, are mainly consists of N-H atoms belonging to isatin group.



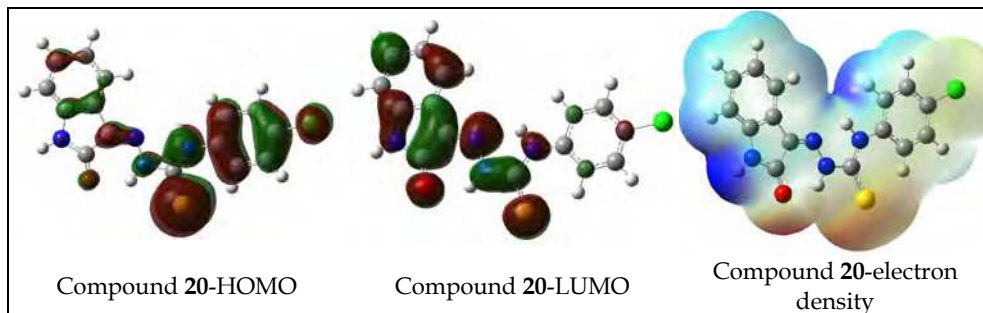


Fig. 3. HOMO, LUMO and electron density calculated at the level of B3LYP/6-311++G(d,p) theory for compounds 18, 5, 19, and 20

### 3.3 IR spectra

Thiosemicarbazones can coordinate with metal ions as neutral ligands (HTSC) or as anionic species (TSC) upon deprotonation at the N(2') (Beraldo & Tosi, 1983, 1986; Borges et al., 1997; Rejane et al., 1999).

Metal acetates with the ligands ( $H_2L$ ) lead to isolation of complexes of formula  $M(HL)_2$  (Rodriguez-Argiuelles et al., 1999). As seen from the C, H, N analyses, the synthesized complexes are with the formula  $M(HL)_2$  (if the ligand is written as  $H_2IPT$ , then complex has the formula of  $M(HIPT)_2$ ) and form 2:1 ligand-to-metal complexes which two of the ligands were anionic.

Infrared absorptions in the range of 4000-400  $cm^{-1}$  have been calculated for 19 with the method, B3LYP/6-31G(d,p), B3LYP/6-311G(d,p) and B3LYP/6-311++G(d,p) and for their Zn(II) and Ni (II) complexes with the method B3LYP/6-31G(d,p), B3LYP/6-311G(d,p), and B3LYP/LanL2DZ. Beside this, infrared frequencies for compounds 18, 5, and 20, and their zinc (II) and nickel (II) complexes have been calculated. Calculated bands and their correspondence experimental values are presented in Tables 7 and 8. Loosing of N12 H band due to deprotonation is one of the main changes (Bresolin et al., 1997).

MO Energy	6-31G(d,p)		6-311G(d,p)		6-311G++(d,p)		LANL2DZ	
	RHF	B3LYP	RHF	B3LYP	RHF	B3LYP	RHF	B3LYP
(a)								
6'	0.18055	0.01472	0.14439	0.00491	0.05089	-0.03326	0.16053	0.00090
5'	0.15887	0.00827	0.13996	-0.00377	0.04569	-0.03286	0.13557	-0.00545
4'	0.13325	-0.01245	0.12068	-0.02526	0.04149	-0.03142	0.11213	-0.02372
3'	0.13102	-0.01563	0.12043	-0.02712	0.03267	-0.01705	0.11212	-0.02547
2'	0.12559	-0.01632	0.11615	-0.02911	0.03241	-0.00870	0.10372	-0.03112
1'	0.04691	-0.08870	0.04111	-0.09642	0.02804	-0.01309	0.02603	-0.10317
1	-0.29966	-0.20958	-0.30438	-0.21286	-0.30635	-0.22160	-0.30530	-0.21316
2	-0.31169	-0.21266	-0.31672	-0.21770	-0.31882	-0.22471	-0.31549	-0.21892
3	-0.32555	-0.21266	-0.32999	-0.24209	-0.33211	-0.24364	-0.33497	-0.24024
4	-0.34287	-0.24654	-0.34749	-0.25866	-0.34886	-0.25832	-0.35162	-0.25603
5	-0.34330	-0.25940	-0.34807	-0.26857	-0.34983	-0.27125	-0.35190	-0.26582
6	-0.34878	-0.26066	-0.35334	-0.26974	-0.35503	-0.27277	-0.35772	-0.26721

<b>(b)</b>								
6'	0.22036	0.07889	0.15398	0.03320	0.05283	-0.00555	0.22904	0.07491
5'	0.21615	0.07539	0.14812	0.02913	0.04826	-0.00929	0.21900	0.07219
4'	0.18048	0.01426	0.14059	0.00407	0.04213	-0.01325	0.16181	0.00122
3'	0.15787	0.00751	0.13494	-0.00274	0.03393	-0.01759	0.13511	-0.00560
2'	0.12486	-0.01671	0.11558	-0.02654	0.03241	-0.03341	0.10324	-0.03120
1'	0.04648	-0.08890	0.04082	-0.09696	0.02768	-0.10207	0.02635	-0.10269
1	-0.29829	-0.20836	-0.30266	-0.21701	-0.30407	-0.21948	-0.30214	-0.21091
2	-0.31042	-0.21108	-0.31499	-0.21922	-0.31631	-0.22241	-0.31288	-0.21568
3	-0.32484	-0.22993	-0.32907	-0.23819	-0.33081	-0.24172	-0.33388	-0.23854
4	-0.34721	-0.24596	-0.35142	-0.25421	-0.35263	-0.25725	-0.35609	-0.25495
5	-0.39928	-0.26914	-0.40313	-0.27761	-0.40410	-0.28176	-0.40838	-0.27693
6	-0.43098	-0.28528	-0.43466	-0.29358	-0.43699	-0.29626	-0.43871	-0.29228
<b>(c)</b>								
6'	0.18135	0.03242	0.14358	0.00235	0.05130	-0.01079	0.17626	0.01936
5'	0.15783	0.00696	0.13850	-0.00421	0.04653	-0.01753	0.13359	-0.00865
4'	0.14350	-0.00375	0.13029	-0.01837	0.04127	-0.02585	0.12023	-0.01588
3'	0.13463	-0.02009	0.12802	-0.02132	0.03540	-0.02825	0.10782	-0.03380
2'	0.12322	-0.02198	0.11434	-0.02779	0.02997	-0.03488	0.09968	-0.03534
1'	0.04323	-0.09503	0.03855	-0.09899	0.02732	-0.10450	0.01959	-0.10946
1	-0.29931	-0.21623	-0.30386	-0.21656	-0.30594	-0.21996	-0.30582	-0.22084
2	-0.30783	-0.21628	-0.31251	-0.22104	-0.31487	-0.22489	-0.32135	-0.22190
3	-0.32430	-0.22239	-0.33168	-0.24187	-0.33378	-0.24588	-0.32368	-0.23349
4	-0.33602	-0.24315	-0.34277	-0.25858	-0.34444	-0.26205	-0.34504	-0.25289
5	-0.34001	-0.25398	-0.34717	-0.26456	-0.34914	-0.26793	-0.34924	-0.26157
6	-0.35686	-0.27301	-0.35596	-0.26571	-0.35765	-0.26889	-0.37209	-0.28058
<b>(d)</b>								
6'	0.17471	0.02265	0.13955	0.01052	0.05007	-0.02179	0.15295	0.00965
5'	0.15375	0.00354	0.13592	-0.00666	0.04981	0.00440	0.12967	-0.01248
4'	0.12806	-0.01734	0.11543	-0.02957	0.04023	0.00291	0.10620	-0.03124
3'	0.12168	-0.02339	0.11423	-0.03312	0.03302	-0.01424	0.10191	-0.03896
2'	0.11948	-0.03026	0.11139	-0.04013	0.02637	-0.00571	0.09757	-0.04281
1'	0.03893	-0.09939	0.03459	-0.10727	0.02552	-0.01692	0.01736	-0.11453
1	-0.30480	-0.22050	-0.30899	-0.22895	-0.31067	-0.23154	-0.31149	-0.22767
2	-0.31382	-0.22213	-0.31803	-0.23052	-0.31983	-0.23281	-0.32058	-0.22812
3	-0.32819	-0.22582	-0.33599	-0.23414	-0.33779	-0.23730	-0.34034	-0.23818
4	-0.33930	-0.24652	-0.34810	-0.25459	-0.34911	-0.25774	-0.35297	-0.25692
5	-0.35484	-0.26768	-0.35724	-0.27708	-0.35800	-0.27925	-0.36610	-0.28266
6	-0.36077	-0.27427	-0.36142	-0.28272	-0.36254	-0.28521	-0.37048	-0.27736
HOMO↔LUMO: 1 ↔ 1'								

Table 6. Calculated values for the highest occupied and the lowest unoccupied molecular orbital energies HOMO and LUMO, and the five molecular orbital energy the nearest frontier orbitals for (a) **18**, (b) **5**, (c) **19**, and (d) **20**

The FT-IR spectra for **19** shows bands at 3298, 3244, 3177, 1703, and 1612  $\text{cm}^{-1}$ , assigned to stretching vibration modes  $\nu\text{N}(8)\text{H}$ ,  $\text{N}(14)\text{H}$ ,  $\nu\text{C}=\text{O}$  and  $\nu\text{C}=\text{N}$ , respectively. Stretching vibration modes of  $\nu\text{N}(8)\text{H}$ ,  $\nu\text{N}(14)\text{H}$ ,  $\nu\text{C}=\text{O}$ , and  $\nu\text{C}=\text{N}$  were found at 3372, 3179, 1703, and 1612  $\text{cm}^{-1}$  for its zinc (II) complex and at 3381, 3271, 1661, and 1614  $\text{cm}^{-1}$  for nickel (II) complex, respectively. The IR peak of  $\text{N}(12)\text{-H}$  of thiosemicarbazide regions at 3283, 3244, 3242, and 3242  $\text{cm}^{-1}$  in the spectra of compounds **18**, **5**, **19**, and **20** ligands are not present in their zinc (II), and nickel (II) complexes, due to proton dissociation, which is the main change (Bresolin et al., 1997). Infrared spectra of the  $\nu(\text{C}=\text{N})$  for compounds **5**, **18**, **19**, and **20** ligands were assigned as 1618, 1620, 1620, and 1622  $\text{cm}^{-1}$ , respectively. In their nickel (II) and zinc (II) complexes, the position of these bands shifted to 1595  $\text{cm}^{-1}$ . On complex formation with nickel (II), and zinc (II),  $\text{C}=\text{S}$  band shifted towards the lower side.

Exp.	6-31G(d,p)		6-311G(d,p)		6-311++G(d,p)		Assignment
	Freq. ( $\text{cm}^{-1}$ )	Intensity	Freq. ( $\text{cm}^{-1}$ )	Intensity	Freq. ( $\text{cm}^{-1}$ )	Intensity	
<b>Compound 19</b>							
3298	3661	75	3642	71	3640	75	$\nu(\text{N}_8\text{H})_{\text{indole}}$
3244	3516	86	3540	96	3543	94	$\nu(\text{N}_{14}\text{H})_{\text{tivo}}$
3177	3432	91	3437	85	3433	84	$\nu(\text{N}_{12}\text{H})_{\text{tivo}}$
			3198	16	3198	13	$\nu(\text{CH})_{\text{ring A combination}}$
3148	3254	12	3198	4	3197	4	$\nu(\text{C}_{26}\text{-H})_{\text{ring C combination}}$
			3194	15	3193	12	$\nu(\text{C}_{25}\text{-H})_{\text{ring C}}, \nu(\text{C}_{26}\text{-H})_{\text{ring C}}, \nu(\text{C}_{27}\text{-H})_{\text{ring C}}, \nu(\text{C}_{29}\text{-H})_{\text{ring C}}$
3071	3216	18	3189	17	3189	13	$\nu(\text{CH})_{\text{ring A combination}}$
3059	3210	27	3186	27	3185	23	$\nu(\text{CH})_{\text{ring C combination}}$
	3207	18	3181	5	3181	5	$\nu(\text{CH})_{\text{ring A combination}}$
	3200	5					$\nu(\text{CH})_{\text{ring A combination}}$
3028	3196	22	3176	6	3175	5	$\nu(\text{C}_{25}\text{-H})_{\text{ring C}}, \nu(\text{C}_{26}\text{-H})_{\text{ring C}}, \nu(\text{C}_{27}\text{-H})_{\text{ring C}}, \nu(\text{C}_{29}\text{-H})_{\text{ring C}}$
	3168	12					$\nu(\text{CH})_{\text{ring C combination}}$
1694	1790	222	1775	257	1758	297	$\nu(\text{C}=\text{O}), \delta(\text{N}_8\text{H}), \delta(\text{N}_{12}\text{H})$
1620							
1594	1675	91	1661	98	1658	94	$\nu(\text{CC})_{\text{ring A combination}}, \delta(\text{N}_8\text{H})$
1539	1661	25	1644	14	1641	15	$\nu(\text{CC})_{\text{ring A combination}}, \delta(\text{N}_{14}\text{C}_{13})$
1492	1652	124					$\nu(\text{CC})_{\text{ring C combination}}, \delta(\text{N}_{14}\text{H})$
			1636	21	1632	15	$\nu(\text{CC})_{\text{ring A combination}}$
1477	1649	16					$\nu(\text{CC})_{\text{ring A combination}}$
			1630	3	1627	3	$\nu(\text{CC})_{\text{ring C combination}}$
1462	1637	175	1623	191	1618	216	$\nu(\text{C}_7\text{-N}_{11}), \delta(\text{N}_{12}\text{H}), \nu(\text{CC})_{\text{ring C combination}}$
1439	1598	750	1544	620	1539	542	$\delta(\text{N}_{14}\text{H}), \delta(\text{CH})_{\text{ring C combination}}$
1412	1541	74					$\delta(\text{CH})_{\text{ring C combination}}, \delta(\text{N}_{12}\text{H}), \delta(\text{N}_{14}\text{H})$
			1525	190	1522	183	$\delta(\text{CH})_{\text{ring A combination}}, \delta(\text{N}_8\text{H}), \delta(\text{N}_{12}\text{H})$

1377	1531	168					$\delta(\text{CH})_{\text{ring A combination}}, \delta(\text{N}_8\text{H}), \delta(\text{N}_{12}\text{H})$
			1522	110	1519	139	$\delta(\text{CH})_{\text{ring C combination}}, \delta(\text{N}_{14}\text{H})$
1341	1522	54	1513	17	1510	17	isatin, $\delta(\text{N}_{12}\text{H})$
1316	1505	143	1494	143	1492	138	$\delta(\text{CH})_{\text{ring A combination}}, \delta(\text{N}_{12}\text{H})$
1298	1487	64	1483	4	1480	4	$\delta(\text{CH})_{\text{ring C combination}}$
1271	1429	148	1418	58	1415	56	$\delta(\text{N}_8\text{H}), \delta(\text{CH})_{\text{ring A combination}}, \delta(\text{N}_{14}\text{H})$
	1407	212	1385	128	1380	136	$\delta(\text{N}_{14}\text{H}), \nu(\text{N}_{12}\text{C}_{13})$
1248	1369	28					$\omega(\text{ring A}), \delta(\text{N}_{14}\text{H})$
1227	1365	39					$\omega(\text{ring A, B, C})$
			1355	72	1353	73	$\omega(\text{isatin})$
1207	1354	23	1312	16	1311	17	$\delta(\text{NH}), \delta(\text{CH})_{\text{ring A combination}}$
1148	1198	895	1189	935	1187	836	$\nu(\text{N-N}) + \delta(\text{ring A}) + \nu(\text{C-N})$
1136	1183	153	1179	212	1177	336	$\nu(\text{C-N}) + \delta(\text{ring A}) + \nu(\text{C-N})$
1101	1127	14	1122	24	1121	28	$\omega(\text{ring A})$
1028	1059	7	1048	9	1047	11	$\omega(\text{phenyl})$
982	1048	3	1021	5	1020	4	$\tau(\text{phenyl ring})$
964	1000	1	1000	4	999	6	$\tau(\text{indole ring})$
941	961	38	955	25	953	23	$\gamma(\text{phenyl ring}) + \omega(\text{N-H})$
903	940	1	932	15	932	15	$\tau(\text{phenyl ring})$
864	889	7	890	7	889	6	$\tau(\text{indole ring})$
793	817	100	823	80	822	81	$\gamma(\text{phenyl ring}) + \gamma(\text{indole ring})$
760	797	45	806	32	796	29	$\gamma(\text{N-H})_{\text{thio}} + \nu(\text{C-C})_{\text{indole ring}} + \tau(\text{indole ring})$
700	771	64	761	33	757	45	$\gamma(\text{indole ring})$
679	763	21	738	54	733	44	$\gamma(\text{N-H})_{\text{thio}} + \gamma(\text{indole ring})$
658	716	97	710	40	707	44	$\gamma(\text{phenyl ring})$
644	697	9	691	18	690	16	$\tau(\text{indole ring}) + \gamma(\text{phenyl ring})$
590	673	18	659	19	658	19	$\tau(\text{phenyl ring}) + \nu(\text{C-S})$
561	592	8	624	13	620	13	$\gamma(\text{C-S})$
503	514	109	517	169	509	107	$\gamma(\text{N-H})_{\text{indole}} + \gamma(\text{N-H})_{\text{thio}}$
480	490	24	458	17	456	19	$\tau(\text{phenyl ring})$
<b>Compound 9</b>							
3372	3667	66	3649	68	3674	37	$\nu(\text{N}_8\text{H})_{\text{indole}}$
	3667	70	3649	70	3674	105	$\nu(\text{N}_8\text{H})_{\text{indole}}$
3179	3615	99	3601	106	3596	98	$\nu(\text{N}_{14}\text{H})_{\text{thio}}$
	3615	105	3601	107	3596	142	$\nu(\text{N}_{14}\text{H})_{\text{thio}}$
3150	3260	28	3242	26	3272	20	$\nu(\text{C}_{25}\text{-H})_{\text{ring C}}$
			3242	105	3272	121	$\nu(\text{C}_{25}\text{-H})_{\text{ring C}}$
3063	3260	116			3266	14	$\nu(\text{CH})_{\text{ring A combination}}$
	3215	10	3198	7	3234	22	$\nu(\text{CH})_{\text{ring A combination}}$
	3214	27					$\nu(\text{CH})_{\text{ring A}} + \nu(\text{CH})_{\text{ring C}}$



3023	3208	77	3198	23	3234	35	$\nu(\text{CH})_{\text{ring A}}$ combination
	3204	14			3203	4	$\nu(\text{CH})_{\text{ring A}}$ combination
	3204	11					$\nu(\text{CH})_{\text{ring A}}$ combination
	3195	29	3191	71			$\nu(\text{CH})_{\text{ring C}}$ combination
	3195	19			3198	3	$\nu(\text{CH})_{\text{ring C}}$ combination
	3190	4	3186	15			$\nu(\text{CH})_{\text{ring C}}$ combination
			3186	10			$\nu(\text{CH})_{\text{ring C}}$ combination
			3178	26			$\nu(\text{C}_{26}\text{-H})_{\text{ring C}}, \nu(\text{C}_{27}\text{-H})_{\text{ring C}}, \nu(\text{C}_{29}\text{-H})_{\text{ring C}}$
			3178	19			$\nu(\text{C}_{26}\text{-H})_{\text{ring C}}, \nu(\text{C}_{27}\text{-H})_{\text{ring C}}, \nu(\text{C}_{29}\text{-H})_{\text{ring C}}$
			3173	4			$\nu(\text{CH})_{\text{ring A}}$ combination
	3165	6	3150	6	3175	4	$\nu(\text{C}_{26}\text{-H})_{\text{ring C}}, \nu(\text{C}_{29}\text{-H})_{\text{ring C}}$
	3165	13	3150	11	3175	18	$\nu(\text{C}_{26}\text{-H})_{\text{ring C}}, \nu(\text{C}_{29}\text{-H})_{\text{ring C}}$
1703	1808	509	1794	559	1690	22	$\nu(\text{C-O})$
	1808	10	1794	7	1690	436	$\nu(\text{C-O})$
1612	1674	184	1652	192	1671	243	$\delta(\text{N}_8\text{H}), \nu(\text{CC})_{\text{ring A}}$ combination
	1674	21	1661	19	1671	48	$\delta(\text{N}_8\text{H}), \nu(\text{CC})_{\text{ring A}}$ combination
	1656	10	1642	6	1649	6	$\delta(\text{N}_{14}\text{H}), \nu(\text{CC})_{\text{ring C}}$ combination
	1648	4	1642	6	1649	5	$\delta(\text{N}_{14}\text{H}), \nu(\text{CC})_{\text{ring C}}$ combination
1595	1648	54	1636	73	1643	48	$\delta(\text{N}_{14}\text{H}), \nu(\text{CC})_{\text{ring C}}$ combination
	1642	16	1631	18	1639	28	$\delta(\text{N}_8\text{H}), \nu(\text{CC})_{\text{ring A}}$ combination
1508	1603	51	1593	42	1582	24	$\nu(\text{N}_{11}\text{C}_7)$
	1602	12	1592	13	1582	66	$\nu(\text{N}_{11}\text{C}_7)$
	1582	5	1576	10			$\delta(\text{N}_{14}\text{H}), \nu(\text{CC})_{\text{ring C}}$ combination
1456	1578	635	1572	591	1573	423	$\delta(\text{N}_{14}\text{H}), \nu(\text{CC})_{\text{ring C}}$ combination
	1537	181	1525	183	1525	10	$\delta(\text{N}_{14}\text{H}), \nu(\text{CC})_{\text{ring C}}$ combination
	1526	12	1516	13	1524	273	$\delta(\text{N}_8\text{H}), \nu(\text{CC})_{\text{ring A}}$ combination
	1510	5	1500	9	1501	15	$\nu(\text{CC})_{\text{ring A}}$ combination
1396	1510	160	1500	179	1501	218	$\nu(\text{CC})_{\text{ring A}}$ combination
	1489	128	1479	90	1478	55	$\delta(\text{N}_{14}\text{H}), \nu(\text{CC})_{\text{ring C}}$ combination
	1488	100	1478	70	1477	76	$\delta(\text{N}_{14}\text{H}), \nu(\text{CC})_{\text{ring C}}$ combination
1338	1464	1142	1446	1189	1451	837	$\nu(\text{N}_{11}\text{C}_7), \nu(\text{N}_{12}\text{C}_{13}), \nu(\text{CH})_{\text{ring C}}$
	1462	2109	1444	2160	1451	1948	$\nu(\text{N}_{11}\text{C}_7), \nu(\text{N}_{12}\text{C}_{13}), \nu(\text{CH})_{\text{ring C}}$
1277	1428	89	1420	129	1431	74	$\delta(\text{N}_8\text{H}), \nu(\text{CC})_{\text{ring A}}$ combination
	1371	41	1363	60	1386	40	$\delta(\text{N}_{14}\text{H}), \nu(\text{CC})_{\text{ring C}}$ combination
1242	1368	81	1359	138	1378	101	$\nu(\text{NH}), \nu(\text{CH})$
	1366	101	1358	119	1377	127	$\delta(\text{N}_8\text{H}), \nu(\text{CC})_{\text{ring A}}$ combination
			1348	17	1373	5	$\delta(\text{N}_{14}\text{H}), \nu(\text{CC})_{\text{ring C}}$ combination
	1361	164	1347	155	1373	95	$\delta(\text{N}_{14}\text{H}), \nu(\text{CC})_{\text{ring C}}$ combination
1178	1324	32	1312	24	1333	45	$\nu(\text{isatin})$
1144	1272	143	1265	138	1300	221	$\rho(\text{indole ring}), \rho(\text{NH})_{\text{semicarbazone}}$
1094	1204	228	1192	222	1273	39	$\sigma(\text{CH})_{\text{indole}} + \nu(\text{C-S})$

1043	1176	443	1166	511	1222	124	$\nu(\text{N-N})+\sigma(\text{CH})_{\text{indole}}$
1007	1122	13	1125	111	1208	123	$\omega(\text{indole ring})$
966	998	64	1116	22	1187	347	$\omega(\text{phenyl ring})$
883	924	5	1000	25	1127	135	$\tau(\text{indole ring})$
833	858	9	995	54	1111	84	$\tau(\text{indole ring})+\rho(\text{C-N})$
802	807	154	855	8	983	92	$\gamma(\text{phenyl ring})$
783	795	62	824	28	974	10	$\gamma(\text{C-N+N-H})$
750	771	46	799	216	894	9	$\nu(\text{C-S})+\nu(\text{C-C})_{\text{indole}}$
690	705	19	768	54	846	18	$\delta(\text{phenyl ring})$
658	696	16	764	19	814	33	$\delta(\text{indole ring})$
611	630	30	706	25	800	121	$\delta(\text{phenyl ring})+\delta(\text{N-H})$
594	605	74	640	19	785	226	$\delta(\text{N-H})+\omega(\text{phenyl ring})$
550	537	19	637	34	725	60	$\delta(\text{N-H})$
<b>Compound 14</b>							
3381	3671	103	3653	103	3680	97	$\nu(\text{N}_8\text{H})_{\text{indole}}$
	3670	49	3653	48	3679	57	$\nu(\text{N}_8\text{H})_{\text{indole}}$
3271	3624	40	3610	40	3606	66	$\nu(\text{N}_{14}\text{H})_{\text{thio}}$
	3624	92	3610	97	3606	81	$\nu(\text{N}_{14}\text{H})_{\text{thio}}$
					3265	5	$\nu(\text{C}_4\text{H})_{\text{ring A}}$
3122	3210	19	3192	17	3230	24	$\nu(\text{CH})_{\text{ring C combination}}$
	3210	44	3192	40	3230	62	$\nu(\text{CH})_{\text{ring C combination}}$
	3209	10	3192	8	3230	20	$\nu(\text{CH})_{\text{ring A combination}}$
3065	3209	57	3192	49	3229	66	$\nu(\text{CH})_{\text{ring A combination}}$
	3200	15	3182	16	3214	13	$\nu(\text{CH})_{\text{ring A combination}}$
	3200	13	3182	12	3214	18	$\nu(\text{CH})_{\text{ring A combination}}$
	3195	43	3178	40	3210	52	$\nu(\text{CH})_{\text{ring C combination}}$
	3173	14	3156	12	3210	4	$\nu(\text{CH})_{\text{ring C combination}}$
					3182	19	$\nu(\text{CH})_{\text{ring C combination}}$
1661	1803	11	1801	24	1686	2	$\nu(\text{isatin}), \nu(\text{N}_{11}\text{C}_7), \nu(\text{C-O})$
	1792	540	1792	620	1678	251	$\nu(\text{isatin}), \nu(\text{N}_{11}\text{C}_7), \nu(\text{C-O})$
					1668	6	$\nu(\text{isatin}), \nu(\text{N}_{11}\text{C}_7), \nu(\text{C-O})$
					1666	534	$\nu(\text{isatin}), \nu(\text{N}_{11}\text{C}_7), \nu(\text{C-O})$
1614	1670	216	1658	240			$\nu(\text{CC})_{\text{ring A combination}}, \delta(\text{N}_8\text{H})$
	1660	32	1645	27	1653	25	$\nu(\text{CC})_{\text{ring C combination}}, \delta(\text{N}_{14}\text{H})$
1595	1659	65	1645	61	1652	87	$\nu(\text{CC})_{\text{ring C combination}}, \delta(\text{N}_{14}\text{H})$
1535	1648	16	1635	25	1643	39	$\nu(\text{CC})_{\text{ring C combination}}, \delta(\text{N}_{14}\text{H})$
	1647	60	1634	80	1642	89	$\nu(\text{CC})_{\text{ring C combination}}, \delta(\text{N}_{14}\text{H})$
	1643	22	1630	16	1640	11	$\nu(\text{CC})_{\text{ring A combination}}, \delta(\text{N}_8\text{H}), \nu(\text{N}_{11}\text{C}_7)$
	1642	13	1629	19	1638	74	$\nu(\text{CC})_{\text{ring A combination}}, \delta(\text{N}_8\text{H}), \nu(\text{N}_{11}\text{C}_7)$
	1626	4	1612	9	1614	27	$\nu(\text{CC})_{\text{ring A combination}}, \delta(\text{N}_8\text{H}), \nu(\text{N}_{11}\text{C}_7)$
1518	1620	48	1566	184	1604	24	$\nu(\text{CC})_{\text{ring A combination}}, \delta(\text{N}_8\text{H}), \nu(\text{N}_{11}\text{C}_7)$

1496	1572	265			1571	139	$\nu(\text{CC})_{\text{ring C combination}}, \delta(\text{N}_{14}\text{H})$
	1569	645	1562	611	1568	539	$\nu(\text{CC})_{\text{ring C combination}}, \delta(\text{N}_{14}\text{H})$
1456	1539	61	1527	69	1527	172	$\nu(\text{CH})_{\text{ring C combination}}, \delta(\text{N}_{14}\text{H})$
	1538	130	1527	133	1526	311	$\nu(\text{CH})_{\text{ring C combination}}, \delta(\text{N}_{14}\text{H})$
	1525	86	1514	81	1512	16	$\nu(\text{isatin}), \nu(\text{N-C-N})$
	1525	68	1514	90	1511	26	$\nu(\text{isatin}), \nu(\text{N-C-N})$
1408	1501	259	1492	303	1490	8	$\nu(\text{CC})_{\text{ring A combination}}, \delta(\text{N}_8\text{H})$
	1501	172	1492	333	1489	145	$\nu(\text{CC})_{\text{ring A combination}}, \delta(\text{N}_8\text{H})$
	1498	220	1488	153	1480	65	$\nu(\text{CC})_{\text{ring A}}, \nu(\text{CC})_{\text{ring C}}, \nu(\text{CH}), \nu(\text{NH})$
	1496	360	1487	228	1480	128	$\nu(\text{CC})_{\text{ring A}}, \nu(\text{CC})_{\text{ring C}}, \nu(\text{N}_{12}\text{C}_{13}), \nu(\text{N}_{11}\text{C}_7)$
1348	1478	790	1465	841	1456	1179	$\nu(\text{CC})_{\text{ring C}}, \nu(\text{N-C-N})$
	1475	687	1463	691	1453	1020	$\nu(\text{CC})_{\text{ring C}}, \nu(\text{N-C-N})$
1315	1422	80	1414	62	1428	147	$\nu(\text{CC})_{\text{ring A combination}}, \delta(\text{N}_8\text{H})$
	1421	87	1414	74	1428	145	$\nu(\text{CC})_{\text{ring A combination}}, \delta(\text{N}_8\text{H})$
	1369	29	1357	31	1385	10	$\nu(\text{CC})_{\text{ring C combination}}, \delta(\text{N}_{14}\text{H})$
1275	1369	54	1356	309	1372	276	$\nu(\text{CC})_{\text{ring A}}, \nu(\text{CC})_{\text{ring C}}, \nu(\text{NH})$
	1364	223	1355	187	1371	141	$\nu(\text{CC})_{\text{ring A}}, \nu(\text{CC})_{\text{ring C}}, \nu(\text{NH})$
	1364	193					$\nu(\text{CC})_{\text{ring A}}, \nu(\text{CC})_{\text{ring C}}, \nu(\text{NH})$
	1356	5			1365	27	$\nu(\text{CH})_{\text{ring C combination}}$
1229	1356	238	1344	278	1365	169	$\nu(\text{CH})_{\text{ring C combination}}$
1165	1309	91	1310	38	1338	43	$\rho(\text{indole ring}), \rho(\text{NH})_{\text{semicarbazone}}$
1143	1272	143	1286	71	1304	96	$\nu(\text{NN})+\sigma(\text{CH})_{\text{indole}}$
1094	1244	10	1265	195	1265	177	$\omega(\text{indole ring})+\omega(\text{N-H})$
1045	1204	228	1237	45	1257	128	$\nu(\text{C}_{\text{phenyl-N}})+\rho(\text{NH})_{\text{semicarbazone}}$
1009	1202	253	1194	693	1229	261	$\omega(\text{phenyl ring})$
937	1176	443	1148	343	1206	45	$\nu(\text{NN})+\sigma(\text{phenyl})$
903	1129	79	1116	107	1189	680	$\rho(\text{indole ring})$
881	1055	3	1029	35	1148	215	$\tau(\text{indole ring})$
839	998	64	915	12	1059	28	$\gamma(\text{indole ring})+\rho(\text{C-N})$
802	943	2	895	13	1026	55	$\gamma(\text{C-N+N-H})$
777	858	9	851	46	951	17	$\delta(\text{indole ring})$
748	807	154	819	19	841	43	$\nu(\text{C-S})+\nu(\text{Ni-N})$
694	795	62	765	45	792	132	$\tau(\text{phenyl ring})$
657	705	19	663	17	631	29	$\delta(\text{N-H})+\omega(\text{phenyl ring})$
421	575	25	572	25	562	25	$\nu(\text{Ni-N})$
327	319	8	362	21	269	5	$\nu(\text{Ni-S})$

Table 7. The experimental and calculated infrared frequencies at the level of B3LYP/6-31G(d,p), B3LYP/6-311G(d,p) and B3LYP/6-311++G(d,p) theory for **19**, at the level of B3LYP/6-31G(d,p), B3LYP/6-311G(d,p), and B3LYP /LANL2DZ theory for its Zn(II) and Ni (II) complexes with their tentative assignment

Compound	Theoretical IR			Experimental IR		
	$\nu(N(8)H)$	$\nu(N(14)H)$	$\nu(N(12)H)$	$\nu(N(8)H)$	$\nu(N(14)H)$	$\nu(N(12)H)$
5	3919	3784	3843	3366	3283	3231
6	3924	-	3885	3379	-	3169
17	3925	-	3882	3296	-	3194
19	3919	3785	3843	3298	3244	3176
9	3922	-	3874	3372	-	3179
14	3924	-	3880	3381	-	3155
18	3919	3787	3858	3366	3242	3166
11	3924	-	3897	3169	-	3402
16	3925	-	3874	3167	-	3394
20	3918	3783	3841	3309	3242	3184
10	3920	-	3873	3348	-	3177
15	3922	-	3879	3383	-	3179
Compound	$\nu(C=O)$	$\nu(C=N)$	$\nu(C=S)$	$\nu(C=O)$	$\nu(C=N)$	$\nu(C=S)$
5	1887	1842	1181	1684	1618	864
6	1890	1817	1124	1688	1595	819
17	1834	1826	1138	1664	1595	823
19	1888	1845	1230	1693	1620	863
9	1898	1828	1124	1703	1595	802
14	1849	1838	1146	1660	1595	802
18	1888	1843	1209	1693	1620	862
11	1894	1828	1121	1690	1599	814
16				1659	1595	818
20	1890	1848	1229	1693	1622	864
10	1899	1830	1124	1695	1600	816
15	1852	1841	1146	1672	1595	817

Table 8. Some important experimental and theoretical IR assignments

The frequency of the  $\nu(C=O)$  vibration shifts to lower energy by ( $\nu = 20\text{-}30\text{ cm}^{-1}$ ) upon coordination as the anion ligands (the frequency of the  $\nu(C=O)$  vibration for compounds **5**, **19**, **18**, and **20** are 1684, 1693, 1693, 1693  $\text{cm}^{-1}$ , whereas for their nickel (II) complexes are 1664, 1660, 1659, and 1672  $\text{cm}^{-1}$ , which may be due to the transfer of a charge from the oxygen to the nickel (Mulliken charge on O10 atom for **19**, its zinc (II) and nickel (II) complexes are 0.359, 0.412, and -0.322, respectively). Thus, it was concluded that nickel (II) complex co-ordinate through the oxygen of (C=O) in the indole ring, and nitrogen, and sulphur atoms, belonging to thiosemicarbazone and C=S groups. In the zinc (II) complexes, no shifting for  $\nu(C=O)$  vibration occurred indicated that only thiosemicarbazone moiety of the compounds **5**, **18**, **19**, and **20** ligands is coordinated in a bidentate way through N and S. In the far-infrared region for zinc (II) complexes, Zn-N, Zn-S vibrations were observed at 422, and 318  $\text{cm}^{-1}$  for compound **6**; 430, and 329 for compound **10**; 420, and 333  $\text{cm}^{-1}$  for compound **11**; 434, and 325  $\text{cm}^{-1}$  for compound **9**; in nickel (II) complexes, Ni-N, Ni-O, and Ni-S were assigned at 420, 374, 316, for compound **17**; 434, 352, 20 $^{-1}$  for compound **15**; 424, 345, 329  $\text{cm}^{-1}$  for compound **16**; 420, 346, 327  $\text{cm}^{-1}$  for compound **14**.

### 3.4 Electronic spectrum

Compounds **5**, **18**, **19**, and **20** were optimized by B3LYP method with 6-31G(d,p), 6-311G(d,p), 6-311++G(d,p), and with density functional theory by using the BP86 hybrid functional with 30% HF exchange (B3P86-30%), and Stevens-Basch-Krauss pseudo potentials with polarized split valence basis sets (CEP-31G\*) (Stevens et al., 1984) and theoretical calculated wave numbers of electronic transitions for compounds **5**, **18**, **19**, and **20** are reported in Tables 9 and 10. Very weak features with oscillator strengths below 0.25 were omitted.

		UV-Visible spectrum data (nm)							
Comp. 18		Experimental	252	268	278	288	296		372
	B3LYP	6-31G(d,p)	219	233	249	264	326		399
		6-311G(d,p)	209	222	236	266	326		401
		6-311++G(d,p)	214	223	227	270	332		407
	BP86	CEP-31G*	210	225	238	255	309		378-349
Comp. 5		Experimental	250	268	278	288	296	364	373
	B3LYP	6-31G(d,p)	210	236	252	267	327		406
		6-311G(d,p)	212	228-237	254	268	328		408
		6-311++G(d,p)	216	242	259	272	334		415
	BP86	CEP-31G*		227	240	257	312		382
Comp. 19		Experimental		258		296		364	370
	B3LYP	6-31G(d,p)	207	249		254-256		355	400
		6-311G(d,p)	210	224-236		264		321	405
		6-311++G(d,p)	213	231-240-256		269		327	412
	BP86	CEP-31G*	216	253-238-226		305		352	382
Comp. 20		Experimental	250	260				368	370
	B3LYP	6-31G(d,p)	208	256-257-262				357	429-402
		6-311G(d,p)	209	251-258-266				358	427-403
		6-311++G(d,p)	209	256-261-269				363	436-409
	BP86	CEP-31G*	236	256-254-245				338	390-382

Table 9. Experimental and theoretical UV assignments for compounds **18**, **5**, **19**, and **20** calculated by using TDB3LYP with the 6-31G(d,p), 6-311G(d,p), 6-311++G(d,p), BP86-CEP-31G\* basis set

The UV visible spectral values, excitation energies, and oscillator strengths were calculated at TDB3LYP levels by using 6-31G(d,p), 6-311Gs(d,p), 6-311++G(d,p) basis sets and TDBP86-CEP-31G\* level for compounds **5**, **18**, **19**, and **20**. There was an agreement between the UV calculations at the level of TDBP86-CEP-31G\* for ligands, and experimental results.

The C=N transitions due to n- $\pi$  for isatin-3-thiosemicarbazones were assigned as 2070 cm<sup>-1</sup> (483 nm) of (Akinchan et al., 2002). This band was found to be 372, 373, 370, 370 nm for compounds **5**, **18**, **19**, and **20**, respectively. At the level of TDBP86-CEP-31G\*, this band for compounds **5**, **18**, **19**, and **20** was found at 382 nm, which arises from 3-1', 2-1', 3-1', and 3-1' transitions. The bands due to  $\pi$ - $\pi^*$  transitions of semicarbazone group for isatin-3-thiosemicarbazone were between the range of 400-286 nm (Akinchan et al., 2002). Band at

305 nm at the level of TDBP86-CEP-31G\* was predicted for compounds **5**, **18**, **19**, and **20**, which arises mainly from 4-1', transitions.

The UV transitions and their excitation energies and oscillator strengths for zinc (II) and nickel (II) complexes of compounds **5**, **18**, **19**, and **20** were calculated by using TDB3LYP with the 6-31G(d,p), 6-311G(d,p), BP86-CEP-31G basis sets. The transitions for nickel (II) complexes were calculated with both multiplicity states, 1 and 3, with two unpaired electrons. The results are summarized in Tables 11-14. The UV spectra, calculated with two unpaired electrons for nickel (II) complexes, were not in agreement with the experimental results. The band assigned at around 372, due to C=N transitions, were observed at 432, and 450 nm in the UV spectra of zinc (II) and nickel (II) complexes, respectively. Band at 434 nm (experimental) for compound **18** was found to be at 436 nm in the calculated of spectra of BP86-CEP-31G. Bands located around 360 nm in zinc (II) complexes and 374 nm in nickel (II) complexes due to ligand LMCT transition, suggested a metal-sulfur bond formation (Akinchan et al., 2002). Nickel (II) complexes showed three transitions around 450, belonging to transition  ${}^3A_{2g} \rightarrow {}^3T_{2g}$  (F), 635 including transition  $A_{2g} \rightarrow {}^3T_{2g}$  (F), and 842 in transition  ${}^3A_{2g} \rightarrow {}^3T_{1g}$  (P), these transitions are characteristic of hexacoordinated nickel (II) complexes.

Compound 18						
6-31G(d,p)	3.11(0.28)E2	3.80(0.35)E5	4.68(0.12)E9	4.98(0.07)E13	5.30(0.07)E16	5.66(0.09)E23
6-311G(d,p)	3.09(0.30)E2	3.80(0.35)E5	4.66(0.11)E9	5.26(0.07)E16	5.58(0.12)E22	5.91(0.10)E26
6-311++G(d,p)	3.04(0.30)E2	3.73(0.32)E5	4.59(0.09)E9	5.47(0.09)E26	5.54(0.07)E28	5.80(0.08)E39
BP86-CEP-31G*	3.28(0.36)E2	3.55(0.08)E3 4.01(0.26)E5	4.86(0.14)E9	5.22(0.10)E11	5.51(0.06)E17	5.88(0.16)E21
Compound 5						
6-31G(d,p)	3.05(0.26)E2	3.78(0.41)E5	4.65(0.11)E6	4.91(0.05)E9	5.26(0.11)E10	5.88(0.10)E18
6-311G(d,p)	3.04(0.28)E2	3.78(0.41)E5	4.63(0.11)E6	4.88(0.04)E9	5.21(0.11)E10	5.43(0.11)E11 5.84(0.09)E18
6-311++G(d,p)	2.99(0.29)E2	3.71(0.39)E5	4.56(0.10)E6	4.79(0.04)E9	5.11(0.11)E12	5.75(0.08)E31
BP86-CEP-31G*	3.24(0.40)E2	3.97(0.34)E5	4.83(0.13)E6	5.16(0.08)E8	5.46(0.10)E10	5.75(0.08)E31
Compound 19						
6-31G(d,p)	3.10(0.27)E3	3.48(0.46)E4	4.88(0.22)E9	4.88(0.18)E10	4.97(0.06)E12	5.11(0.10)E15 5.98(0.08)E26
6-311G(d,p)	3.06(0.34)E2	3.86(0.37)E5	4.69(0.16)E10	5.26(0.08)E16	5.51(0.06)E21	5.90(0.14)E25
6-311++G(d,p)	3.01(0.34)E2	3.79(0.34)E5	4.61(0.14)E10	4.84(0.05)E14	5.16(0.06)E18	5.37(0.04)E23 5.80(0.16)E35
BP86-CEP-31G*	3.24(0.41)E2	3.52(0.07)E3	4.06(0.29)E5	4.88(0.20)E9	5.21(0.08)E14	5.50(0.08)E17 5.74(0.06)E18
Compound 20						
6-31G(d,p)	2.80(0.06)E2	3.08(0.26)E3	3.47(0.49)E4	4.72(0.29)E9	4.81(0.08)E10	4.83(0.17)E11 5.96(0.10)E28
6-311G(d,p)	2.90(0.06)E2	3.07(0.28)E3	3.47(0.48)E4	4.65(0.29)E9	4.80(0.024)E12	4.93(0.06)E13 5.92(0.09)E28
6-311++G(d,p)	2.84(0.05)E2	3.03(0.28)E3	3.41(0.46)E4	4.60(0.28)E9	4.74(0.018)E12	4.90(0.10)E14 5.93(0.10)E41
BP86-CEP-31G*	3.17(0.12)E2	3.24(0.32)E3	3.66(0.42)E4	4.83(0.24)E9	4.88(0.013)E10	5.05(0.25)E11 5.24(0.10)E13

Table 10. TDB3LYP method with the 6-31G(d,p), 6-311G(d,p), 6-311++G(d,p) basis sets and TDBP86-CEP-31G\* excitation energies in eV for compounds **18**, **5**, **19**, and **20**, and Oscillator Strengths (in Parenthesis)

Compound <b>11</b>	-	254	268	288	296	360	434
6-31G(d,p)			249	361	364	436-441	457
6-311G(d,p)			251	363	365	436-439	453
CEP-31G			239		356-352	422-420	436
Compound <b>6</b>	-	254	268	290	296	364	434
6-31G(d,p)		211	250	359	365	437	444
6-311G(d,p)		213-212	252	361	366	439-436	450
CEP-31G			241		355-350	435-423-420	
Compound <b>9</b>	250	-	258	-	302	308	444
6-31G(d,p)	228		243-264		401-403	450	461-463
6-311G(d,p)	245		250-265		400-401	450-462	474-478
CEP-31G	240-234		254		388	438-428	461-457-453
Compound <b>10</b>	-	-	260		300	312	444
6-31G(d,p)	249-253-256		270		406-406	455	475-479
6-311G(d,p)	252-261		271		404-404	465	481-484
CEP-31G	260-248-241-236				435-390	448-443	461-460

Table 11. Experimental and theoretical UV assignments for compounds **11**, **6**, **9**, and **10** calculated by using TDB3LYP with the 6-31G(d,p), 6-311G(d,p), BP86-CEP-31G basis set

Comp. <b>16</b>	254	262	296	374	450	635	842
6-31G(d,p)	251	-	346	363-374	408-419	659	729
311G(d,p)	255	266	342-308	365-355	423-412	657-617	-
CEP-31G	248-244	293-261	345-344-300	387-384	473-445	606	-
6-311G(d,p) <sup>(1)</sup>	-	-	346-346-344	386-381	490-434-432	-	-
CEP-31G <sup>(1)</sup>	-	-	330-330	367-366	415-411	476	-
Comp. <b>17</b>	244	264	292	378	450	636	832
6-31G(d,p)	247-231	252	344	375-361	459-418-406	659	731
6-311G(d,p)	229-247	265	340-353-364	409-421	456	620-658	-
CEP-31G	246-241-237	301-265	343-342-332	386-382	475-447	614	-
6-311G(d,p) <sup>(1)</sup>	-	-	386-382	403-392	486-418	-	-
CEP-31 <sup>(1)</sup>	253-248-242	263	366-363-359-328-327	-	416-412	-	-
Comp. <b>14</b>	-	260	300	414	435	636	826
6-31G(d,p)	-	250-252-263	280-310	374-379-392	421-430	604-652	743
6-311G(d,p)	-	253-262-270-288-305	306-311-368	368-392	432-421	622	663
CEP-31G	253-248-248-239-236	298-287-265	370-321	413-410-397	486-448	614	-
6-311G(d,p) <sup>(1)</sup>	-	-	406-342-341	447-420-419	510	-	-
CEP-31G <sup>(1)</sup>	-	288	354	425-405-401	494	-	-
[Ni(HICPT) <sub>2</sub> ]	-	264	300	410	-	637	883
6-31G(d,p)		286-310	374	433	-	-	747
6-311G(d,p)	309	310	374	384			666

CEP-31G	256-255- 248-239	321-294- 289-268	394-371	413-409	485	-	613
6-311G(d,p) <sup>(1)</sup>	-	-	406-374-370	448-425-422	511	-	-
CEP-31G <sup>(1)</sup>	-	288	405-401-354	425	493	-	-

(1) triplet state

Table 12. Experimental and theoretical UV assignments for compounds **16**, **17**, **14**, and **15** calculated by using TDB3LYP with the 6-31G(d,p), 6-311G(d,p), BP86-CEP-31G basis set

Compound 11							
6-31G(d,p)	3.11(0.28)E2	3.80(0.35)E5	4.68(0.12)E9	4.98(0.07)E13	5.30(0.07)E16	5.66(0.09)E23	
6-311G(d,p)	3.09(0.30)E2	3.80(0.35)E5	4.66(0.11)E9	5.26(0.07)E16	5.58(0.12)E22	5.91(0.10)E26	
6-311++G(d,p)	3.04(0.30)E2	3.73(0.32)E5	4.59(0.09)E9	5.47(0.09)E26	5.54(0.07)E28	5.80(0.08)E39	
CEP-31G	3.24(0.41)E2	4.06(0.29)E5	4.88(0.19)E9	5.20(0.08)E14	5.50(0.08)E17	5.74(0.06)E18	
Compound 6							
6-31G(d,p)	3.05(0.26)E2	3.78(0.41)E5	4.65(0.11)E6	4.91(0.05)E9	5.26(0.11)E10	5.88(0.10)E18	
6-311G(d,p)	3.04(0.28)E2	3.78(0.41)E5	4.63(0.11)E6	4.88(0.04)E9	5.21(0.11)E10	5.43(0.11)E11 5.84(0.09)E18	
6-311++G(d,p)	2.99(0.29)E2	3.71(0.39)E5	4.56(0.10)E6	4.79(0.04)E9	5.11(0.11)E12	5.75(0.08)E31	
CEP-31G	3.24(0.40)E2	3.97(0.34)E5	4.83(0.13)E6	5.16(0.08)E8	5.46(0.10)E10	5.75(0.08)E31	
Compound 9							
6-31G(d,p)	3.10(0.27)E3	3.48(0.46)E4	4.88(0.22)E9	4.88(0.18)E10	4.97(0.06)E12	5.11(0.10)E15 5.98(0.08)E26	
6-311G(d,p)	3.06(0.34)E2	3.86(0.37)E5	4.69(0.16)E10	5.26(0.08)E16	5.51(0.06)E21	5.90(0.14)E25	
6-311++G(d,p)	3.01(0.34)E2	3.79(0.34)E5	4.61(0.14)E10	4.84(0.05)E14	5.16(0.06)E18	5.37(0.04)E23 5.80(0.16)E35	
CEP-31G	3.24(0.41)E2	3.52(0.07)E3	4.06(0.29)E5	4.88(0.20)E9	5.21(0.08)E14	5.50(0.08)E17 5.74(0.06)E18	
Compound 10							
6-31G(d,p)	2.88(0.06)E2	3.08(0.26)E3	3.47(0.49)E4	4.72(0.29)E9	4.81(0.08)E10	4.83(0.17)E11 5.96(0.10)E28	
6-311G(d,p)	2.90(0.06)E2	3.07(0.28)E3	3.47(0.48)E4	4.65(0.29)E9	4.80(0.024)E12	4.93(0.06)E13 5.92(0.09)E28	
6-311++G(d,p)	2.84(0.05)E2	3.03(0.28)E3	3.41(0.46)E4	4.60(0.28)E9	4.74(0.018)E12	4.90(0.10)E14 5.93(0.10)E41	
CEP-31G	3.17(0.12)E2	3.24(0.32)E3	3.66(0.42)E4	4.83(0.24)E9	4.88(0.013)E10	5.05(0.25)E11 5.24(0.10)E13	

Table 13. TDB3LYP method with the 6-31G(d,p), 6-311G(d,p), 6-311++G(d,p) basis sets and TDBP86-CEP-31G excitation energies in eV for compounds **11**, **6**, **9**, **10**, and Oscillator Strengths (in Parenthesis)

Compound 16							
6-31G(d,p)	1.70(0.06)E3 1.88(0.02)E4	2.95(0.12)E11	3.31(0.15)E13	3.40(0.14)E16 3.41(0.24)E19	3.58(0.10)E22	4.92(0.21)E76	
311G(d,p)	1.88(0.03)E3 2.01(0.07)E4	2.93(0.11)E12	3.01(0.11)E13	3.39(0.26)E18 3.49(0.09)E21	3.62(0.11)E24 4.03(0.08)E33	4.65(0.26)E60 4.92(0.21)E76	
CEP-31	2.04(0.08)E5	2.62(0.06)E8 2.79(0.07)E9	3.20(0.13)E12 3.22(0.12)E13	3.58(0.25)E17 3.60(0.18)E18	4.12(0.08)E27 4.23(0.10)E29	4.74(0.08)E45 4.98(0.18)E53 5.07(0.30)E58	
6-311G(d,p) <sup>(1)</sup>	2.53(0.06)E13	2.86(0.15)E19	2.87(0.07)E20 3.21(0.12)E28 3.24(0.07)E30	3.58(0.19)E36 3.58(0.08)E37	3.60(0.10)E39	3.82(0.10)E51	



CEP-31 <sup>(1)</sup>	2.60(0.10)E10	2.98(0.14)E19	3.01(0.08)E20	3.37(0.18)E27	3.38(0.06)E28	3.75(0.15)E39 3.76(0.20)E40
<b>Compound 17</b>						
6-31G(d,p)	1.70(0.06)E3 1.88(0.02)E4	2.70(0.06)E9 2.96(0.13)E11	3.05(0.09)E13 3.29(0.15)E16 3.60(0.18)E22	4.91(0.23)E54	5.00(0.18)E57	5.34(0.17)E67
311G(d,p)	1.88(0.04)E3 1.99(0.06)E4	2.71(0.06)E9 3.02(0.13)E11	3.03(0.10)E13 3.38(0.17)E18 3.54(0.12)E21	3.64(0.11)E24	4.67(0.18)E47	5.02(0.27)E57 5.41(0.10)E69
CEP-31	2.02(0.08)E5	2.61(0.06)E8 2.77(0.06)E9	3.21(0.14)E12 3.24(0.10)E13 3.61(0.20)E17	3.62(0.18)E18 3.73(0.09)E20 4.11(0.08)E27	4.67(0.09)E37	5.03(0.42)E46 5.14(0.13)E49 5.21(0.14)E52
6-311G(d,p) <sup>(1)</sup>	2.55(0.07)E15	2.96(0.06)E26	3.07(0.08)E30 3.14(0.08)E32	3.27(0.05)E36 3.20(0.06)E38	3.62(0.22)E47	3.64(0.77)E48
CEP-31 <sup>(1)</sup>	3.24(0.14)E19 3.19(0.08)E20	3.19(0.11)E25 3.41(0.05)E28	3.18(0.10)E30 3.06(0.19)E37 3.0(0.18)E38	3.20(0.06)E62 3.06(0.17)E67	4.99(0.06)E71	5.10(0.17)E76
<b>Compound 14</b>						
6-31G(d,p)	1.67(0.08)E3 1.90(0.02)E5 2.05(0.01)E7	2.88(0.21)E11 2.95(0.09)E13	3.16(0.13)E17 3.26(0.12)E19 3.31(0.11)E21	4.00(0.11)E33 4.42(0.12)E50 4.70(0.09)E61	4.91(0.12)E72	4.97(0.19)E75
311G(d,p)	1.87(0.07)E3 1.99(0.04)E4	2.72(0.06)E9 2.88(0.19)E12	2.99(0.10)E13 3.15(0.16)E18 3.37(0.22)E23	3.98(0.09)E33 4.05(0.09)E37	4.29(0.11)E44	4.59(0.10)E57 4.72(0.08)E62 4.90(0.33)E73
CEP-31	2.02(0.10)E5 2.55(0.07)E8	2.77(0.05)E9 2.99(0.16)E11 3.02(0.32)E12	3.12(0.12)E15 3.35(0.07)E16	3.85(0.13)E25 4.15(0.11)E29 4.30(0.14)E33	4.67(0.10)E43 4.89(0.30)E51 4.99(0.12)E56 4.99(0.17)E57	5.13(0.08)E61 5.16(0.16)E62 5.23(0.35)E68
6-311G(d,p) <sup>(1)</sup>	2.43(0.10)E13	3.26(0.10)E19	2.95(0.25)E27	2.96(0.29)E28	3.05(0.12)E29	
CEP-31 <sup>(1)</sup>	2.51(0.09)E10	2.91(0.09)E21	3.06(0.36)E23	3.09(0.38)E24	3.50(0.06)E36	4.31(0.11)E58
<b>Compound 15</b>						
6-31G(d,p)	1.66(0.08)E3	2.86(0.22)E11	3.30(0.16)E21	3.99(0.13)E34	4.32(0.13)E48	4.66(0.10)E63 4.70(0.12)E67
311G(d,p)	1.86(0.06)E5	3.22(0.22)E18	3.30(0.16)E21	3.57(0.10)E23	3.99(0.13)E34	4.00(0.34)E37
CEP-31	2.02(0.10)E5	2.56(0.08)E8 3.00(0.17)E11 3.02(0.34)E12	3.14(0.08)E15 3.33(0.10)E16 3.86(0.16)E25	4.15(0.11)E29 4.28(0.14)E31 4.61(0.07)E41	4.83(0.06)E49 4.85(0.12)E51 4.87(0.36)E52	4.95(0.10)E57 4.99(0.11)E59 5.17(0.31)E65
6-311G(d,p) <sup>(1)</sup>	2.42(0.10)E13	3.27(0.11)E19	2.91(0.24)E27	3.42(0.34)E28	3.04(0.08)E29	3.31(0.09)E33
CEP-31 <sup>(1)</sup>	2.51(0.09)E10	3.51(0.09)E10	2.91(0.09)E21	3.06(0.36)E23	3.08(0.38)E24	3.04(0.06)E36

<sup>(1)</sup> triplet state

Table 14. TDB3LYP method with the 6-31G(d,p), 6-311G(d,p), 6-311++G(d,p) basis sets and TDBP86-CEP-31G excitation energies in eV for compounds **16**, **17**, **14**, **15**, and Oscillator Strengths (in Parenthesis)

### 3.5 NMR spectra

Experimental and calculated theoretical NMR parameters for compounds **5**, **18**, **19**, and **20** were shown in Table 15. Geometrical optimization of studied ligands were performed at the level of B3LYP/6-311G(d,p), and B3LYP/6-311++G(d,p). NMR Chemical shifts were predicted from Gauge-Independent Atomic Orbital (GIAO) calculations at the same level of theory at DMSO solution with both gas phase optimization and DMSO optimization. Theoretically calculated <sup>1</sup>H-NMR parameters are generally in agreement with experimental results, except deviation in N8-H of isatin ring, and N14-H of thiosemicarbazone group.

The correlations between theoretical, and experimental NMR results, calculated with B3LYP/6-311, B3LYP/6-311++ level of theory are 97.6%, and 98.2% and at gas phase; 96.9%, 96.4%, in DMSO solution (but optimization was in gas phase), and at the B3LYP/6-311++ level of theory 96.9% in DMSO solution (and also optimisation in DMSO solution) for compound **18**. Although the experimental proton signal of N12-H of isatin group for compounds **5**, **18**, **19**, and **20** was 12.64, 12.57, 12.81 and 12.85, and theoretical one was  $\delta$  12.37, 12.21, 12.55, 12.51 in the DMSO solution at the level of B3LYP/6-311++G(dip) theory.

	Atoms	6-311-G(d,p)		6-311++G(d,p)		6-311++G(d,p)	Exp,
		gas	DMSO <sup>a</sup>	gas	DMSO <sup>a</sup>	DMSO	
Compound <b>18</b>	C1-H	7.30	7.53	7.24	7.66	7.55	7.01
	C2-H	6.99	7.13	7.01	7.31	7.17	7.31
	C3-H	6.76	7.08	6.78	7.30	7.11	6.91
	C4-H	7.38	7.49	7.53	7.63	7.53	7.63
	C21-H	4.53	4.51	4.67	4.71	4.52	4.86
	C21-H	4.53	4.51	4.67	4.71	4.52	
	C25-H	7.66	7.78	7.75	8.06	7.80	7.32-7.36
	C26-H	7.66	7.78	7.75	8.05	7.80	7.32-7.36
	C27-H	7.62	7.76	7.75	8.05	7.77	7.32-7.36
	C29-H	7.62	7.76	7.72	8.05	7.77	7.32-7.36
	C31-H	7.58	7.74	7.54	7.88	7.75	7.23
	N8-H	6.16	6.80	6.43	7.86	6.88	9.77
	N12-H	12.27	12.17	12.62	12.46	12.37	12.64
	N14-H	6.84	7.23	7.17	7.44	7.16	11.18
Compound <b>5</b>	C1-H	7.37	7.60	7.40	7.82	7.62	7.10
	C2-H	7.14	7.30	7.18	7.50	7.33	7.36
	C3-H	6.80	7.11	6.77	7.27	7.14	6.93
	C4-H	7.66	7.81	7.74	7.98	7.85	7.74
	C24-H	4.42	4.22	4.50	4.41	4.35	4.19
	C26-H	2.36	2.12	2.39	2.18	1.98	1.92
	C26-H	0.98	1.23	1.00	1.27	1.31	1.54-1.44
	C27-H	1.53	1.50	1.53	1.52	1.53	1.35-1.26
	C27-H	1.77	1.81	1.79	1.85	1.84	1.77
	C31-H	1.25	1.34	1.29	1.39	1.33	1.14
	C31-H	1.69	1.68	1.70	1.71	1.70	1.64
	C29-H	1.54	1.52	1.55	1.56	1.54	1.35-1.26
	C29-H	1.83	1.88	1.82	1.88	1.88	1.77
	C25-H	1.98	1.96	2.03	2.04	1.92	1.92
	C25-H	1.31	1.55	1.36	1.60	1.45	1.54-1.44
	N8-H	6.18	6.81	6.47	7.90	6.89	8.85
N12-H	12.19	12.05	12.41	12.23	12.21	12.57	
N14-H	7.06	7.55	7.28	7.70	7.44	11.20	

Compound 19	C1-H	7.39	7.63	7.46	7.87	7.64	7.12
	C2-H	7.15	7.29	7.21	7.51	7.33	7.38
	C3-H	6.83	7.14	6.78	7.29	7.18	6.95
	C4-H	7.69	7.84	7.71	8.03	7.88	7.78
	C25-H	7.47	7.56	7.58	7.86	7.58	7.63
	C26-H	7.47	7.56	7.58	7.86	7.81	7.63
	C27-H	7.61	7.80	7.67	8.04	7.80	7.44
	C29-H	7.61	7.80	7.67	8.04	7.81	7.44
	C31-H	7.58	7.79	7.56	7.93	7.58	7.28
	N8-H	6.22	6.86	6.46	7.89	6.94	10.83
	N12-H	12.40	12.32	12.61	12.45	12.55	12.81
N14-H	8.65	9.08	8.80	9.45	9.03	11.26	
Compound 20	C1-H	7.43	7.63	7.34	7.73	7.65	7.12
	C2-H	9.42	7.33	7.22	7.52	7.37	7.38
	C3-H	6.85	7.14	6.81	7.30	7.17	6.95
	C4-H	7.78	7.95	7.88	8.11	7.98	7.77
	C26-H	6.80	7.24	6.90	7.44	7.24	7.67
	C29-H	7.33	7.55	7.43	7.87	7.55	7.49
	C27-H	7.46	7.54	7.55	7.85	7.57	7.49
	C25-H	9.91	9.75	9.98	9.84	9.77	7.67
	N8-H	6.25	6.86	6.54	7.94	6.94	10.86
	N12-H	12.40	12.33	12.71	12.58	12.51	12.85
	N14-H	9.42	9.77	9.76	10.10	9.74	11.27

<sup>a</sup> Optimisation were calculated in the gas phase and Theoretical NMR shifting were calculated in the DMSO solution

Table 15. Experimental and theoretical NMR shifting for compounds **18**, **5**, **19**, and **20** calculated by using B3LYP with the 6-311G(d,p), 6-311++G(d,p) basis set for gas and DMSO phase

The proton signal of N8-H group seen at  $\delta$  9.77, 8.85, 10.83, 10.88, respectively, in the  $^1\text{H}$ -NMR spectrum for compounds **5**, **18**, **19**, and **20**, also appeared in the spectrum of their zinc (II) complexes at  $\delta$  10.81, 10.80, 11.01, and 11.06, respectively. The upfield shift was due to the lack of intermolecular hydrogen bonding in its corresponding complex (Akinchan et al., 2002). A stronger hydrogen-bond interaction will shorten the O-H distance, will elongate the N-H distance, and will also cause a significant deshielding of the proton leading to a further downfield NMR signal (De Silva et al., 2007). The peak due to N12-H in the  $^1\text{H}$ -NMR spectra of compounds **5**, **18**, **19**, and **20** disappeared in their corresponding complexes.

The experimental and theoretical NMR results of compounds **11**, **6**, **9**, and **10** are shown in Table 16. Geometrical optimizations of above mentioned studied complexes were performed by using the B3LYP method, and 6-31G(d,p), 6-311G(d,p) standard basis sets at the gas phase, and DMSO solution. The calculated peak, due to N12-H in the  $^1\text{H}$ -NMR spectra of compounds **5**, **18**, **19**, and **20** disappears in their corresponding zinc (II) complexes, as the calculation was performed by considering the corresponding ligand, deprotonated from N12 belong to thiosemicarbazone group in its complex form.

	Atoms	6-311G(d,p)		6-31G(d,p)	6-311G(d,p)	Experimental	
		gas	DMSO <sup>a</sup>	gas	DMSO		
Compound 11	C1-H	7.63	7.21	7.79	-	6.95-7.40	
	C2-H	6.97	6.84	7.23	-		
	C3-H	7.11	6.55	7.27	-		
	C4-H	7.53	7.68	8.02	-		
	C25-H	7.80	7.77	7.97	-		
	C29-H	7.95	7.66	8.09	-		
	C31-H	7.84	7.53	7.99	-		
	C27-H	7.86	7.54	8.01	-		
	C22-H	7.78	7.47	7.88	-		
	C21-H	6.15	6.41	6.25	-		4.76
	C21-H	4.17	4.00	4.30	-		
	N8-H	7.38	5.98	8.11	-	10.81	
	N14-H	6.33	5.33	6.91	-	9.26	
	Compound 6	C1-H	7.14	7.14	7.73	7.38	6.90-8.30
C2-H		6.73	6.73	7.17	6.85		
C3-H		6.51	6.51	7.23	6.89		
C4-H		7.43	7.43	7.82	7.43		
C24-H		4.80	4.80	4.98	4.64		
C26-H		2.41	2.41	2.34	2.08	1.15-2.34	
C26-H		1.05	1.05	1.52	1.26		
C27-H		1.69	1.69	1.96	1.76		
C27-H		1.72	1.72	1.81	1.51		
C31-H		1.69	1.69	1.87	1.69		
C31-H		1.25	1.25	1.59	1.31		
C29-H		1.82	1.82	2.06	1.90		
C29-H		1.64	1.64	1.85	1.59		
C25-H		1.24	1.24	1.69	1.40		
C25-H		2.03	2.03	2.21	2.06		
N8-H		5.97	5.97	8.06	6.69		10.80
N14-H		5.30	5.30	6.83	5.65		8.77
Compound 9	C1-H	7.61	7.79	7.43	7.43	7.01-8.11	
	C2-H	6.93	7.22	6.84	6.84		
	C3-H	7.13	7.31	6.98	6.98		
	C4-H	7.60	8.08	7.60	7.60		
	C26-H	7.49	7.51	7.24	7.24		
	C29-H	7.83	7.97	7.67	7.67		
	C31-H	7.56	7.76	7.43	7.43		
	C27-H	7.94	8.11	7.83	7.83		
	C25-H	10.10	10.22	10.14	10.14		
	N8-H	8.26	8.63	7.63	7.63		11.01
	N14-H	7.55	8.27	6.90	6.90	10.68	

Compound 10	C1-H	7.61	7.22	7.81	7.43	7.03-8.08
	C2-H	6.92	6.74	7.21	6.82	
	C3-H	7.13	6.59	7.32	6.97	
	C4-H	7.54	7.70	8.01	7.64	
	C25-H	7.43	6.77	7.51	7.15	
	C29-H	7.67	7.29	7.83	7.48	
	C27-H	7.79	7.63	7.97	7.65	
	C26-H	10.09	10.21	10.28	10.13	
	N8-H	8.20	7.25	8.59	7.55	11.06
	N14-H	7.55	6.15	8.28	6.88	10.74

<sup>a</sup> Optimisation were calculated in the gas phase and Theoretical NMR shifting were calculated in the DMSO solution

Table 16. Experimental and theoretical NMR shifting for compounds **11**, **6**, **9**, and **10** calculated by using B3LYP with the 6-31G(d,p), 6-311G(d,p) basis set for gas and DMSO phase

### 3.6 Antibacterial activity

All the compounds **1-16** were tested against the two Gram-positive bacterial strains i.e. *Staphylococcus aureus* and *Bacillus subtilus*, and four Gram-negative bacterial strains i.e. *Escherichia coli*, *Shigella flexnari*, *Pseudomonas aeruginosa*, and *Salmonella typhi*, according to the literature protocol (Becke, 1993). The results were compared with the standard drug imipenem and shown in Table 17.

Compound Name	Escherichia coli	Bacillus subtilus	Shigella flexnari	Staphylococcus aureus	Pseudomonas aeruginosa	Salmonella typhi
1	00	00	00	00	00	00
2	00	00	00	00	00	00
3	00	00	00	00	00	00
4	00	00	00	00	00	00
5	00	00	00	00	00	00
6	00	00	00	00	00	00
7	00	00	00	00	00	00
8	00	00	00	00	00	00
9	00	00	00	00	00	00
10	00	00	00	00	00	00
11	00	00	00	00	00	00
12	00	00	00	00	00	00
13	00	00	00	00	00	00
14	00	00	00	00	00	00
15	00	00	00	00	00	00
16	00	00	00	00	00	00
SD* Imipenem	30	33	27	33	24	25

Table 17. Antibacterial activity for *Escherichia coli*, *Shigella flexnari*, *Pseudomonas aeruginosa*, and *Salmonella typhi*

### 3.7 Antifungal activity

All the compounds **1-16** were also tested against *Candida albicans*, *Aspergillus flavus*, *Microsporium canis*, *Fusarium solani*, and *Candida glabrata*, according to the literature protocol (Lee et al., 1988) and found that compounds showed a varying degree of percentage inhibition. These results were compared with the standard drugs miconazole and amphotericin B, as shown in Table 18.

Compound Name	<b>1</b>	<b>2</b>	<b>3</b>	<b>4</b>	<b>5</b>	<b>6</b>	<b>7</b>	<b>8</b>	SD
C. albicans	0	0	0	0	0	0	0	0	110
A. flavus	20	0	20	0	40	0	0	0	20
M. canis	50	60	00	60	30	0	0	80	98
F. Solani	20	0	30	40	10	0	25	30	73
C. glabrata	0	0	0	0	0	0	0	0	101
Compound Name	<b>9</b>	<b>10</b>	<b>11</b>	<b>12</b>	<b>13</b>	<b>14</b>	<b>15</b>	<b>16</b>	SD
C. albicans	0	40	0	0	0	0	0	0	110
A. flavus	30	0	20	0	20	0	0	0	20
M. canis	20	0	20	20	70	50	20	50	98
F. Solani	05	0	0	40	40	20	0	0	73
C. glabrata	0	0	0	0	0	0	0	0	101

Table 18. Antifungal activity for *Candida albicans*, *Aspergillus falvus*, *Microsporium canis*, *Fusarium solani*, and *Candida galbrata*

Compounds **1**, **14**, **16**, **8**, and **13** exhibited activity against *Microsporium canis* with 50, 50, 50, 80, and 70% inhibition, respectively. Compounds **4**, **12**, and **13** showed a moderate inhibition against *Fusarium solani* with a percentage inhibition of 40, 40, and 40%, respectively. Compound **5** demonstrated activity an against *Aspergillus flavus* (40% inhibition). Compound **10** was found to be active against *Candia albicans* with 40% inhibition.

Table 18 shows results of antifungal assay on compounds **1-16** (concentration used 200 µg/mL of DMSO, and Percentage Inhibition). All the compounds in this series showed non-significant activity against all the bacteria.

### 4. Acknowledgement

The financial support for this study was provided by the TUBITAK Fund (Project Number: 108T974), and the High Education Commission of Pakistan.

### 5. References

Agrawal, K.C. & Sartorelli, A.C. (1978). The chemistry and biological activity of  $\alpha$ -(N)-heterocyclic carboxaldehyde Thiosemicarbazones. *Prog. Med. Chem.*, Vol. 15, pp. (321-356), ISSN: 0079-6468.

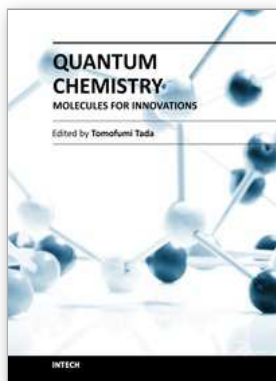
- Ajaiyeoba, E.O.; Rahman, A. & Choudhary, M.I. (1988). Preliminary antifungal and cytotoxicity studies of extracts of *Ritchiea capparoides* var. *Longipedicellata*. *J. Ethnopharm.*, Vol: 62, No. 3, pp. (243-246), ISSN: 0378-8741.
- Akinchan, N.T.; Drozdowski, P.M. & Holzer, W. (2002). Syntheses and spectroscopic studies on zinc(II) and mercury(II) complexes of isatin-3-thiosemicarbazone. *J. Mol. Struct.*, Vol. 641, No. 1, pp. (17-22), ISSN: 0022-2860.
- Bal, T.R.; Anand, B.; Yogeewari, P. & Sriram, D. (2005). Synthesis and evaluation of anti-HIV activity of isatin  $\beta$ -thiosemicarbazone derivatives. *Bioorg. Med. Chem. Lett.*, Vol. 15, No. 20, pp. (4451-4455), ISSN: 0960-894X.
- Becke, A.D. (1993). Density-functional thermochemistry. III. The role of exact exchange. *J. Chem. Phys.*, Vol. 98, No. 7, pp. (5648-5652), ISSN: 0021-9606.
- Beraldo, H. & Tosi, L. (1983). Spectroscopic studies of metal complexes containing  $\pi$ -delocalized sulfur ligands. The resonance raman spectra of the iron(II) and iron (III) complexes of the antitumor agent 2-formylpyridin thiosemicarbazone. *Inorg. Chim. Acta.*, Vol. 75, pp. (249-257), ISSN: 0020-1693.
- Beraldo, H. & Tosi, L. (1986). Spectroscopic studies of metal complexes containing  $\pi$ -delocalized sulfur ligands. The pre-resonance Raman spectra of the antitumor agent 2-formylpyridine thiosemicarbazone and its Cu(II) and Zn(II) complexes. *Inorg. Chim. Acta.*, Vol. 125, No. 3, pp. (173-182), ISSN: 0020-1693.
- Borges, R.H.U.; Paniago, E.; Beraldo, H. (1997). Equilibrium and kinetic studies of iron(II) and iron(III) complexes of some  $\alpha$ (N)-heterocyclic thiosemicarbazones. Reduction of the iron(III) complexes of 2-formylpyridine thiosemicarbazone and 2-acetylpyridine thiosemicarbazone by cellular thiol-like reducing agents. *J. Inorg. Biochem.*, Vol. 65, No. 4, pp. (267-275), ISSN: 0162-0134.
- Bresolin, L.; Burrow, R.A.; Hörner, M.; Bermejo, E. & Castineiras A. (1997). Synthesis and crystal structure of di [ $\mu$ -acetato](2-acetylpyridine<sup>4</sup> N-ethylthiosemicarbazonato)zinc(II)]. *Polyhedron*, Vol. 16, No. 23, pp. (3947-3951), ISSN: 0277-5387.
- Boon, R. (1997). Antiviral treatment: from concept to reality. *Antiviral Chem. Chemother.*, Vol: 8, pp. (5-10), ISSN: 0956-3202.
- Casas, J.S.; Castineiras, A.; Sanchez, A.; Sordo, J.; Vazquez-Lopez, A.; Rodriguez-Argiuelles, M.C. & Russo U. (1994). Synthesis and spectroscopic properties of diorganotin(IV) derivatives of 2,6-diacetylpyridine bis(thiosemicarbazone). Crystal structure of diphenyl[2,6-diacetylpyridine bis(thiosemicarbazonato)]tin(IV) bis(dimethylformamide) solvate. *Inorg. Chem. Acta.*, Vol. 221, no. 1-2, pp (61-68), ISSN: 0020-1693.
- Casas, J.S.; García-Tasende, M.S.; Maichle-Mössner, C.; Rodríguez-Argiuelles, M.C.; Sánchez, A.; Sordo, J.; Vázquez-López, A.; Pinelli, S.; Lunghi, P. & Albertini, R. (1996). Synthesis, structure, and spectroscopic properties of acetato (dimethyl) (pyridine-2-carbaldehydethiosemicarbazonato)tin(IV) acetic acid solvate, [SnMe<sub>2</sub> (PyTSC)(OAc)].HOAc. Comparison of its biological activity with that of some structurally related diorganotin(IV) bis(thiosemicarbazonates). *J. Inorg. Biochem.*, Vol. 62, No. 1, pp. (41-55), ISSN: 0162-0134.

- Casas, J.S.; Castiñeiras, A.; Rodríguez-Argüelles, M.C.; Sánchez, A.; Sordo, J.; Vázquez-López, A. & Vázquez-López, E.M. (2000). Reactions of diorganotin(IV) oxides with isatin 3- and 2-thiosemicarbazones and with isatin 2,3-bis(thiosemicarbazone): influence of diphenyldithiophosphinic acid (isatin = 1*H*-indole-2,3-dione). *J. Chem. Soc. Dalton Trans.*, Vol. 2000, No. 22, pp. (4056-4063), ISSN: 1477-9226.
- Daisley, R.W. & Shah, V.K. (1984). Synthesis and antibacterial activity of some 5-Nitro-3-phenyliminoindol-2(3*H*)-ones and their *N*-mannich bases. *J. Pharm. Sci.*, Vol. 73, No. 3, pp. (407-409), ISSN: 1520-6017.
- De Silva, N.W.S.V.N. & Albu, T.V. (2007). A theoretical investigation on the isomerism and the NMR properties of thiosemicarbazones. *Central Eur. J. Chem.*, Vol. 5, No. 2, pp. (396-419), ISSN: 1644-3624.
- Frisch, M.J.; Trucks, G.W.; Schlegel, H.B.; Scuseria, G.E.; Robb, M.A.; Cheeseman, J.R.; Montgomery, J.A.; Vreven, T.; Kudin, K.N.; Burant, J.C.; Millam, J.M.; Iyengar, S.S.; Tomasi, J.; Barone, V.; Mennucci, B.; Cossi, M.; Scalmani, G.; Rega, N.; Petersson, G.A.; Nakatsuji, H.; Hada, M.; Ehara, M.; Toyota, K.; Fukuda, R.; Hasegawa, J.; Ishida, M.; Nakajima, T.; Honda, Y.; Kitao, O.; Nakai, H.; Klene, M.; Li, X.; Knox, J.E.; Hratchian, H.P.; Cross, J.B.; Bakken, V.; Adamo, C.; Jaramillo, J.; Gomperts, R.; Stratmann, R.E.; Yazyev, O.; Austin, A.J.; Cammi, R.; Pomelli, C.; Ochterski, J.W.; Ayala, P.Y.; Morokuma, K.; Voth, G.A.; Salvador, P.; Dannenberg, J.J.; Zakrzewski, V.G.; Dapprich, S.; Daniels, A.D.; Strain, M.C.; Farkas, O.; Malick, D.K.; Rabuck, A.D.; Raghavachari, K.; Foresman, J.B.; Ortiz, J.V.; Cui, Q.; Baboul, A.G.; Clifford, S.; Cioslowski, J.; Stefanov, B.B.; Liu, G.; Liashenko, A.; Piskorz, P.; Komaromi, I.; Martin, R.L.; Fox, D.J.; Keith, T.; Al-Laham, M.A.; Peng, C.Y.; Nanayakkara, A.; Challacombe, M.; Gill, P.M.W.; Johnson, B.; Chen, W.; Wong, M.W.; Gonzalez, C. & Pople, J.A. (2004). Gaussian 03; Revision B.05, *Gaussian, Inc.*, Wallingford CT.
- Gunesdogdu-Sagdinc, S.; Köksoy, B.; Kandemirli, F. & Bayari, S.H. (2009). Theoretical and spectroscopic studies of 5-fluoro-isatin-3-(*N*-benzylthiosemicarbazone) and its zinc(II) complex. *J. Mol. Struct.*, Vol. 917, No. 2-3, pp. (63-70), ISSN: 0022-2860.
- Hill, M.G.; Mann, K.R.; Miller, L.L. & Penneau, J.F. (1992). Oligothiophene cation radical dimers. An alternative to bipolarons in oxidized polythiophene. *J. Am. Chem. Soc.*, Vol. 114, No. 7, pp. (2728-2730), ISSN: 0002-7863.
- Gorelsky, S.I. & Lever, A.B.P. (2001). Electronic structure and spectra of ruthenium diimine complexes by density functional theory and INDO/S. Comparison of the two methods. *J. Organomet. Chem.*, Vol. 635, No. 1-2, pp. (187-196), ISSN: 0022-328X.
- Gorelsky, S.I. (2009). AOMix: Program for Molecular Orbital Analysis, *University of Ottawa*, <http://www.sg-chem.net/>.
- Ivanov, V.E.; Tihomirova, N.G. & Tomchin, A.B. (1988). *Zh. Obshch. Khim.*, Vol. 58, No. , pp. (2737-2743), ISSN: 1070-3632.
- Kandemirli, F.; Arslan, T.; Karadayı, N.; Ebenso, E.E. & Köksoy, B. (2009). Synthesis and theoretical study of 5-methoxyisatin-3-(*N*-cyclohexyl)thiosemicarbazone and its Ni(II) and Zn(II) complexes. *J. Mol. Struct.*, Vol. 938, No. 1-3, pp. (89-96), ISSN: 0022-2860.



- Kandemirli, F.; Arslan, T.; Koksoy, B. & Yilmaz, M. (2009). Synthesis, Characterization and Theoretical Calculations of 5-Methoxyisatin-3-thiosemicarbazone Derivatives. *J. Chem. Soc. Pakistan*, Vol. 31, No. , pp. (498-504), ISSN: 0253-5106.
- Karali, N.; Gürsoy, A.; Kandemirli, F.; Shvets, N.; Kaynak, F.B.; Özbey, S.; Kovalishyn, V. & Dimoglo, A. (2007). Synthesis and structure–antituberculosis activity relationship of 1*H*-indole-2,3-dione derivatives. *Bioorg. Med. Chem.*, Vol. 15, No. 17, pp. (5888-5904), ISSN: 0968-0896.
- Lee, C.; Yang, W. & Parr, R.G. (1988). Development of the Colle-Salvetti correlation-energy formula into a functional of the electron density. *Phys. Rev. B*, Vol. 37, No. 2, pp. (785-789), ISSN: 1098-0121.
- Medvedev, A.E.; Sandler, M. & Glover, V. (1998). Interaction of isatin with type-A natriuretic peptide receptor: possible mechanism. *Life Sci.*, Vol. 62, No. 26, pp. (2391-2398), ISSN: 0024-3205.
- Pandeya, S.N. & Dimmock, J.R. (1993). Recent evaluations of thiosemicarbazones and semicarbazones and related compounds for antineoplastic and anticonvulsant activities. *Pharmazie*, Vol. 48, No. 9, pp. (659-666), ISSN: 0031-7144.
- Pandeya, S.N.; Sriram, D.; De Clercq, E.; Pannecouque, C. & Witvrouw, M. (1998). Anti-HIV activity of some mannich bases of Isatin derivatives. *Ind. J. Pharm. Sci.*, Vol. 60, No. 4, pp. (207-212), ISSN: 0250-474X.
- Pandeya, S.N.; Sriram D; Nath G; De Clercq E (1999). Synthesis, antibacterial, antifungal and anti-HIV activities of Schiff and Mannich bases derived from isatin derivatives and *N*-[4-(4'-chlorophenyl)thiazol-2-yl] thiosemicarbazide. *Eur. J. Pharm. Sci.*, Vol. 9, No. 1, pp. (25-31), ISSN: 0928-0987.
- Pirrung, M.C.; Pansare, S.V.; Sarma, K.D.; Keith, K.A. & Kern, E.R. (2005). Combinatorial Optimization of Isatin- $\beta$ -Thiosemicarbazones as Anti-poxvirus Agents. *J. Med. Chem.*, Vol. 48, No. 8, pp. (3045-3050), ISSN: 0022-2623.
- Piscopo, B.; Diurno, M.V.; Godliardi, R.; Cucciniello, M. & Veneruso, G. (1987). Studies on heterocyclic compounds Indole-2,3-dione derivatives variously substituted hydrazones with antimicrobial activity. *Boll. Soc. Ital. Biol. Sper.*, Vol. 63, No. , pp. (827-830), ISSN: 0037-8771.
- Rahman, A.; Choudhary, M.I. & Thomsen, W.J. (2001). Antibacterial Assays, *Bioassay Techniques for Drug Development*, Rahman, A., pp. (14-22), Harwood Academic Publishers, ISBN: 90-5823-051-1, The Netherlands.
- Rejane LL; Teixeira LRS; Carneiro TMG; Beraldo H (1999) Nickel(II), Copper(I) and Copper(II) Complexes of Bidentate Heterocyclic Thiosemicarbazones. *J. Braz. Chem. Soc.*, Vol. 10, No. 3, pp. (184-188), ISSN: 0103-5053.
- Rodríguez-Argüelles, M.C.; Sánchez, A.; Ferrari, M.B.; Fava, G.G.; Pelizzi, C.; Pelosi, G.; Albertini, R.; Lunghi, P. & Pinelli, S. (1999). Transition-metal complexes of isatin- $\beta$ -thiosemicarbazone. X-ray crystal structure of two nickel complexes. *J. Inorg. Biochem.*, Vol. 73, No. 1-2, pp. (7-15), ISSN: 0162-0134.
- Ronen, D.; Sherman, L.; Bar-Nun, S. & Teitz, Y. (1987). *N*-methylisatin- $\beta$ -4',4'-diethylthiosemicarbazone, an inhibitor of Moloney leukemia virus protein production: characterization and in vitro translation of viral mRNA. *Antimicrob. Agents Ch.*, Vol. 31, No. 11, pp. (1798-1802), ISSN: 0066-4804.

- Sherman, L.; Edelstein, F.; Shtacher, G.; Avramoff, M. & Teitz, Y. (1980). Inhibition of Moloney Leukaemia Virus Production by *N*-methylisatin- $\beta$ -4':4'-diethylthiosemicarbazone. *J. Gen. Virol.*, Vol. 46, No. 1, pp. (195-203), ISSN: 0022-1317.
- Stevens, W.J.; Basch, H. & Krauss, M. (1984). Compact effective potentials and efficient shared-exponent basis sets for the first- and second-row atoms. *J. Chem. Phys.*, Vol. 81, No. 12, pp. (6026-6033), ISSN: 0021-9606.



## Quantum Chemistry - Molecules for Innovations

Edited by Dr. Tomofumi Tada

ISBN 978-953-51-0372-1

Hard cover, 200 pages

**Publisher** InTech

**Published online** 21, March, 2012

**Published in print edition** March, 2012

Molecules, small structures composed of atoms, are essential substances for lives. However, we didn't have the clear answer to the following questions until the 1920s: why molecules can exist in stable as rigid networks between atoms, and why molecules can change into different types of molecules. The most important event for solving the puzzles is the discovery of the quantum mechanics. Quantum mechanics is the theory for small particles such as electrons and nuclei, and was applied to hydrogen molecule by Heitler and London at 1927. The pioneering work led to the clear explanation of the chemical bonding between the hydrogen atoms. This is the beginning of the quantum chemistry. Since then, quantum chemistry has been an important theory for the understanding of molecular properties such as stability, reactivity, and applicability for devices. This book is devoted for the theoretical foundations and innovative applications in quantum chemistry.

### How to reference

In order to correctly reference this scholarly work, feel free to copy and paste the following:

Fatma Kandemirli, M. Iqbal Choudhary, Sadia Siddiq, Murat Saracoglu, Hakan Sayiner, Taner Arslan, Ayşe Erbay and Baybars Köksoy (2012). Quantum Chemical Calculations for some Isatin Thiosemicarbazones, Quantum Chemistry - Molecules for Innovations, Dr. Tomofumi Tada (Ed.), ISBN: 978-953-51-0372-1, InTech, Available from: <http://www.intechopen.com/books/quantum-chemistry-molecules-for-innovations/quantum-chemical-calculations-for-some-isatin-thiosemicarbazones>

# INTECH

open science | open minds

### InTech Europe

University Campus STeP Ri  
Slavka Krautzeka 83/A  
51000 Rijeka, Croatia  
Phone: +385 (51) 770 447  
Fax: +385 (51) 686 166  
[www.intechopen.com](http://www.intechopen.com)

### InTech China

Unit 405, Office Block, Hotel Equatorial Shanghai  
No.65, Yan An Road (West), Shanghai, 200040, China  
中国上海市延安西路65号上海国际贵都大饭店办公楼405单元  
Phone: +86-21-62489820  
Fax: +86-21-62489821

© 2012 The Author(s). Licensee IntechOpen. This is an open access article distributed under the terms of the [Creative Commons Attribution 3.0 License](#), which permits unrestricted use, distribution, and reproduction in any medium, provided the original work is properly cited.